

Behavior of shear connectors joined by direct fastening

Z.W. Shan and R.K.L. Su*

Department of Civil Engineering, The University of Hong Kong, Pokfulam Road,

Hong Kong, PRC

Abstract

Direct fastening is an effective method to quickly and easily connect two steel components. However, the behaviors of this kind of connection have been rarely studied and there is no direct reference to them in current design specifications. Therefore, it is now timely to investigate the properties and behavior of this type of connection. In this paper, 11 coupons were tested at room temperature and 24 coupons were tested at high temperatures and after fire, to examine the deterioration of the mechanical properties of the steel. Moreover, 24 samples that were connected by direct fastening were tested at high temperatures and post fire conditions to study the deterioration in the shear strength of the fastener at different temperatures. Furthermore, 100 samples that were connected by direct fastening were tested in an ambient temperature to examine the effect of the number of fasteners, fastener spacing, fastener arrangement, knurled fasteners and protuberance. Based on the tested results, a modified expression for the yield strength of this kind of connection was proposed. Besides that, the bearing resistance versus displacement (BRVD) of the connections was numerically modeled and plotted into a simple curve based on the three key parameters of yield strength, effectiveness stiffness and ultimate displacement.

Keywords: High temperature; post-fire; direct fastening; bearing resistance; knurled

* Corresponding author. Tel.: +852 2859 2648

E-mail address: klsu@hku.hk (RKL Su)

fasteners.

1. Introduction

Steel structures have been widely used globally because they are labor and time efficient, and easy to construct. The type of connection is a key factor for consideration when joining different steel structural parts because it affects not only the behavior but also the speed of construction and the construction cost of steel structures. Currently, the most popular connection methods are bolting and welding. Bolting involves the drilling of holes so holes are pre-drilled on steel plates and then bolts are placed through these holes. However, this process means that on-site assembly is a challenging task if sufficient construction tolerance has not been allowed. As for welding, the parts that are to be joined are subjected to heat and subsequently fused. However, the process depends on the weather as cold temperatures might cause weld failure, and also depends on workmanship and the type of equipment used. Overhead welding and welding thin steel plates are extremely challenging tasks which require a certain degree of skill. Moreover, welding can cause residual stress which leads to failure in the form of the bending or distortion of the steel members. Bolting could be preferable, as regards to residual stress.

Compared to the two conventional methods of connecting steel structural parts discussed above, direct fastening which is developed by Hilti Corporation is more user friendly. Unique hardened fasteners are driven into steel material by using a powder-actuated gun or battery-actuated gun. Direct fastening has many applications. According to the Hilti direct fastening technical guide [1], direct fastening can be used to fasten thin metal sheets, such as roofs and floor decks, and thicker steel members, for example metal brackets. Additionally, this method can be used to connect built-up

steel members.

Steel plates are joined by using different anchoring mechanisms in which fasteners are driven into the steel plates. These anchoring mechanisms include clamping, keying, fusing and soldering, among which clamping and keying are especially important because the former causes protuberance and keying allows interlocking, which are considered to significantly affect the yield strength of this type of connection.

However, this joining method has not been fully studied in the literature. Lu et al. [2] conducted an experimental study and proposed design equations for screwed connections, but these are not applicable to connections joined by direct fastening owing to the different anchoring mechanisms. After that, Lu et al. [3] studied the behavior of connections joined by powder-actuated fastening in cold-formed steel sheeting at ambient and elevated temperatures. The effect of protuberance when the nails were driven into the material was also discussed which the authors found is a contributor to the transfer of shear load through the connections. They called this shot nailed connections. Following that, they proposed design guidelines for shot nailed connections because no other similar standards are available for higher temperatures [4]. Nevertheless, there are some limitations in their work. First, they only focused on connections joined with one fastener. Second, only very thin steel sheets were taken into consideration. Third, only one type of fastener – a knurled fastener, was used. Besides that, other studies have also carried out testing but for connections joined by bolting and screwing that were subjected to high temperatures; see [5-7]. The main conclusion from their tests is that there is deterioration of the mechanical properties of the connections under elevated temperatures. Hence, in this paper, only the deterioration behavior of steel material and shear resistance of the fasteners are tested at high temperatures and after exposure to fire.

Furthermore, there are no direct equations in the current codes, such as EN-1993-1-8 [8], ANSI/AISC 360-10 [9] and AS 4100 [10], for designing this type of connection. Equations for predicting the maximum bearing resistance of bolted and screwed connections are provided in these specifications. However, these equations cannot be applied to estimate the maximum bearing resistance (yield strength) of connections joined by direct fastening without any modifications, which will be discussed and elaborated in this paper.

The keying mechanism can only be used with knurled fasteners. Hence, two different types of fasteners, X-S 14 B3 MX and X-U 16 with the material tensile strength of 2000 MPa, are used to investigate the effect of keying, as shown in Figure 1. It can be observed in the figure that X-S 14 B3 MX is not knurled, while X-U 16 is knurled. Similar to screws, these fasteners have a decreasing diameter from the head to the tip. One hundred connections using these two types of fasteners were tested in an ambient temperature and the effects of fastener type, number of fasteners, fastener arrangement, fastener spacing and protuberance were taken into consideration. Besides that, 11 coupons were tested at room temperature and 24 coupons and 24 connections were tested at high temperatures and after exposure to fire conditions. Based on the test results, reduction and residual factors were developed to quantify the deterioration behavior of the steel material and fasteners under high temperatures and exposure to fire conditions. Modified equations for evaluating the yield strength of these connections were then formulated, and the bearing resistance versus displacement (BRVD) was plotted as a simple curve based on three key parameters for the connections.

2. Testing properties of coupons

2.1. Test setup and coupon samples

The test setup is shown in Figure 2, which consists of an MTS 810 material testing system that was equipped with an MTS 653.04 three heating zone furnace. A safety cover and ventilation system were used to control the contamination from the heating process. The maximum heating temperature and rate of heating of the furnace were 1400 °C and 100 °C/min, respectively. Heat was generated with three pairs of independently-controlled heating elements, in which three internal thermocouples were used to measure the air temperature. Two external thermocouples were placed on the surface of the sample to measure its physical temperature. An MTS 632.54F-11 axial extensometer with a gauge length of 25 mm was used to measure the extension displacement. The measured force and strain were collected by using a data acquisition system. The tested coupon samples were prepared based on ASTM E 21 [11]. The dimensions of the coupon samples are shown in Figure 3. In total, details of the 35 samples including 11 coupons for testing in an ambient temperature are presented in Table 1, 12 coupons for testing at high temperatures and 12 coupons for testing post-fire are summarized in Table 2.

2.2. Test procedures

The steady state method was applied for both high temperature and post-fire testing. The samples were heated to the target temperature and then kept constant. After that, the samples were loaded until a load drop of 80% of the maximum load occurred. Li and Young [12] examined the effect of the heating rate on the mechanical properties of steel, which they found was negligible. Therefore, a heating rate of 50 °C/min was used in this study for both high temperature and post-fire testing. For the former, the samples were heated to the target temperature and then maintained at that temperature for 10 minutes [23, 24] to ensure that the sample was evenly heated.

During the process, the lower grip of the material test system was loosened to ensure that there was free extension of the samples. For the latter, one additional step in addition to those in the high temperature test was carried out, which was to cool the samples in air to an ambient temperature after they were heated to the target temperature and then kept constant for 10 minutes .

2.3. Test results

2.3.1. Definition of yield stress and ultimate stress

Under elevated temperature and post fire, the strengths of steel would be reduced. In general, if a specific yield plateau appears in the stress versus strain curve, the yield stress is defined as the lowest value in the yield plateau. Otherwise, it is obtained according to the 2% strain (see Figure 4), which is consistent with that in ANSI/AISC 360-16 [9]. The ultimate stress is the peak stress on the stress versus strain curve.

2.3.2. High temperature testing

The experimental data obtained from the tests conducted at high temperatures in Tan [13] who examined Q 235 mild steel with a nominal yield strength of 235 MPa were used as a comparison. Q 235 is labeled in accordance with Chinese steel code GB50017 [14], which is the equivalent of structural steel S235 in EN-1993-1-1 [15]. The test results [13] of S235 together with those S275 and S355 from this study were utilized to investigate the mechanical properties of steel under high temperature. The reduction factor was used to quantify the reduction properties of the steel under high temperatures. The reduction factors of the elastic modulus, yield strength and ultimate strength were plotted in Figure 5 and listed in Tables 3 and 4. It is obvious that the mechanical properties deteriorate with temperature, which may be induced by the

change in microscope structure of steel when the temperature is higher than a specific value. The recommended reduction factors in EN-1993-1-2 [16] which are derived based on transient state tests and ANSI/AISC 360-16 [9] are also plotted in Figure 5 for comparison purposes. The recommended values provided in EN-1993-1-2 [16] and ANSI/AISC 360-16 [9] can be used to predict the reduction factors of the elastic modulus. To predict the reduction factors of the yield strength derived by using steady state method, modified values were proposed in Eq. (1):

$$Rd_y = \begin{cases} 1.0, & 20^\circ C \leq T < 200^\circ C \\ 1.0 - \frac{0.9}{500}(T - 200), & 200^\circ C \leq T < 700^\circ C \end{cases} \quad (1)$$

Furthermore, the reduction factor for ultimate strength is missing in both EN-1993-1-2 [16] and ANSI/AISC 360-16 [9]. In this study, Eq.(2) is proposed based on limited tested data and available data in a previous study [13] to supplement the current specifications.

$$Rd_u = \begin{cases} 1.0, & 20^\circ C \leq T < 300^\circ C \\ 1.76 - 0.76 \frac{T}{300}, & 300^\circ C \leq T < 600^\circ C \\ 0.69 - 0.15 \frac{T}{200}, & 600^\circ C \leq T \end{cases} \quad (2)$$

2.3.3. Post-fire testing

Mild steel is a popular metal because it is versatile, relatively easy to produce, and inexpensive. Therefore, mild steel is widely used for buildings, machinery, fencing, and a variety of other uses. Since mild steel is popular, their mechanical properties post-fire also have an important role in the design of steel structures. However, there are few studies that have examined the mechanical properties of mild steel post-fire. Furthermore, only the specifications in BS 5950 [17] provide some recommended residual values for the mechanical properties of mild steel post-fire. Therefore,

experiments were conducted and previously tested data were selected to determine the residual factors that can be used to quantify the mechanical properties of mild steel post fire. The results from existing studies [18-21] on the mechanical properties of mild steel post-fire were plotted in Figure 6 and summarized in Tables 5 and 6.

Figure 6 shows that the mechanical properties have almost no influence when the steel is subjected to a temperature less than 400 °C. Then, the mechanical properties begin to deteriorate with further increases in temperature. The strength deterioration is not serious when compared with that under high temperature. This is because cooling process produces positive effect in the recovery of the mechanical properties of steel after fire. According to BS 5950 [17], the residual factors shown in Figure 6 are overly conservative. Hence, the values should be updated for more accuracy to properly evaluate the residual factors. In the following proposed residual factors, the criterion of 95% confidence interval was utilized.

For the residual factors of the elastic modulus, the updated recommended values were given by:

$$R_{S_E} = \begin{cases} 1.0, & 20^{\circ}\text{C} \leq T < 350^{\circ}\text{C} \\ 1.0 - 0.07 \frac{T - 350}{500}, & 350^{\circ}\text{C} \leq T < 1000^{\circ}\text{C} \end{cases} \quad (3)$$

For the residual factors of the yield strength, the updated recommended values were given by:

$$R_{S_y} = \begin{cases} 1.0, & 20^{\circ}\text{C} \leq T < 400^{\circ}\text{C} \\ 1.0 - 0.2 \frac{T - 400}{600}, & 400^{\circ}\text{C} \leq T < 1000^{\circ}\text{C} \end{cases} \quad (4)$$

For the residual factors of the ultimate strength, the updated recommended values were given by:

$$R_{S_u} = \begin{cases} 1.0, & 20^{\circ}\text{C} \leq T < 400^{\circ}\text{C} \\ 1.0 - 0.18 \frac{T - 400}{600}, & 400^{\circ}\text{C} \leq T < 1000^{\circ}\text{C} \end{cases} \quad (5)$$

3. Testing properties of fasteners

3.1. Test setup, procedures and samples

The shear strength of two types of fasteners with same tensile strength of 2000 MPa, X-S 14 B3 MX and DX 16, was tested in high temperatures and post-fire. The heating rate was 50 °C/min and the loading rate was 0.5 mm/min. The test setup is shown in Figure 2 and the testing procedures for the samples subjected to high temperatures and post-fire conditions are the same as those used for testing the properties of the coupons. The dimensions of the tested samples are shown in Figure 7. These dimensions are chosen to accommodate the length of the furnace and material testing system. Besides that, the selected dimensions of steel plates need to ensure that fastener shear fracture is the only failure mode to measure the shear strength of the fasteners at various temperatures. To achieve this, the maximum bearing resistance of the connection should be higher than the shear strength of the fastener multiplied by a factor of 1.5. Both the maximum bearing resistance of the connection and shear strength of the fastener were determined in accordance with EN 1993-1-8. 12 samples were tested under high temperature and another 12 samples were tested post fire.

3.2. Test results

All the samples were failed in shear fracture of fasteners. Two representative shear resistance versus displacement curves are shown in Figure 8. The labeling is consistence with that in Section 4.3 except that ‘A’ is replaced by a specific temperature and ‘PF’ was added to depict samples post fire. For samples under high temperature, shear fracture happens in a strain softening way owing to the shear deformation of fastener shank while this happens abruptly for samples post fire. The shear strength of fasteners can be obtained directly from the shear resistance versus displacement curves. The reduction strength factors of the two types of fasteners that are subjected to high temperatures were shown in Table 7 and plotted in Figure 9. It

can be observed from the figure that the shear strength is not reduced when the temperature is less than 250 °C. Then as the temperature is increased, the shear strength decreases accordingly. The recommended reduction strength factors by Hilti Corporation [1] were also indicated in Figure 9. The reduction strength factors were obtained through a regression analysis as follows:

$$Rd_f = \begin{cases} 1.0, & 20^\circ C \leq T < 250^\circ C \\ 3.57e^{(-T/201.5)} - 0.05, & 250^\circ C \leq T < 700^\circ C \end{cases} \quad (6)$$

The residual strength factors of the two types of fasteners in the post-fire conditions were shown in Table 8 and plotted in Figure 10. The residual strength starts to decline at a temperature of 250 °C until 650 °C . With further increases in temperature, there is no longer a trend of decline of the shear strength. The proposed residual strength factor was given by:

$$Rs_f = \begin{cases} 1.0, & 20^\circ C \leq T < 250^\circ C \\ 1.32 - 0.14 \frac{T}{100}, & 250^\circ C \leq T < 650^\circ C \\ 0.40, & 650^\circ C \leq T \end{cases} \quad (7)$$

4. Testing connections

4.1. Test setup and procedure

The MTS 810 material testing system (Figure 2) which has a maximum capacity of 350 kN was used to test the properties of the connection samples in an ambient temperature. Two gaskets were inserted between the upper and lower grips to allow the single shear of the connection samples (Figure 11). The rate of loading was 0.5 mm/min. The testing for each connection sample was terminated when the bearing resistance was reduced to less than 20% of the maximum bearing resistance to investigate the post-peak behavior of the connection samples.

4.2. Connection sample design

There are four failure modes of the connection samples, including shear-out failure, net section and fastener shear fractures, and bearing failure. Shear-out failure and net section fractures are not considered in designs but can be prevented by considering the values of the end distance and edge distance. Therefore, the minimum end distance and edge distance of both $1.2 d_0$ (diameter of fastener hole) are given in accordance with EN-1993-1-8 [8]. $3.0 d_0$ for end distance and $2.0 d_0$ for edge distance were proposed to ensure that bearing failure happens [2]. Yan and Young [5] utilized $3.0 d_0$ for both end distance and edge distance but few samples failed in net section tension failure. In this paper, a more conservative value of $5 d_0$ was adopted for the end distance and edge distance to prevent shear-out failure and net section fracturing.

To investigate the effect of the number of fasteners and fastener arrangement, 6 types of connection samples were designed in which the thickness of the connected steel plate is 3 mm and thickness of the base steel plate varies from 2 mm to 6 mm; see Figure 12. 40 samples connected by the X-S 14 B3 MX fastener were pre-drilled to eliminate the effects of protuberance on the connected steel plate. Another 60 samples were jointed using fastener of X-U 16 with no pre-drilled process. In total, 100 connection samples were tested under ambient temperature with no repetition.

4.3. Connection sample labeling

Six variables were investigated in this paper. To clearly differentiate the different connection samples, they were labeled as shown in Table 9. Take for example, S275-A-4-5-6(30)-L: S275 denotes that the nominal yield strength of the steel material is 275 MPa; 'A' denotes that the sample is tested at room temperature; '4' represents the nominal diameter of the fastener; '5' signifies the thickness of the base

steel plate; '6(30)' means that there are 6 fasteners with a fastener spacing of 30 mm; and 'L' means that the arrangement of these 6 fasteners is parallel to the load direction or Type 5 as illustrated in Figure 12.

4.4. Failure modes and failure behavior

Two kinds of failure modes - bearing failure and shear fracture failure, were examined in the tests. These two failure modes were shown in Figure 13. Similar to the bearing failure in bolted or screwed connections, this failure is shown with enlarged nail holes due to large plastic deformation and the bulging of the material around the fastener holes, which can be observed in Figures 13(a) and 13(b).

The plotted BRVD curves of the connections were presented in Figure 14. The BRVD curve for S275-A-4-4-1 is used as an example to clarify the failure process of this connection. In the initial stage, the steel plate is in an elastic region and the resistance force linearly increases with the displacement. When the steel material begins to yield, there is no longer a linear relationship between the load and displacement. In this stage, the load increases nonlinearly with displacement, after which the bearing resistance remains approximately constant with increase in displacement. During this stage, the holes on the steel plates are obviously enlarged and fasteners are not normal to the steel plates any more. As a result, a pull-out force is generated in the fasteners. The connection cannot resist any force when the pull-out force exceeds the friction force that is found between the fasteners and steel plates. Thereafter, the bearing resistance decreases to zero on the BRVD curve in Figure 14, which corresponds to an obvious inclination or the final rotation of the fasteners as shown in Figures 13(a) and 13(b). As for the failure process of the connections joined with more than one type of fastener, pull-out failure does not occur simultaneously but sequentially. Therefore, there are inflection point shown on the BRVD curves of

the connections with more than one fastener; see Figure 14.

4.5. Ductility behavior

Ductility capacity of connections joined by direct fastening is defined as the ultimate displacement to yield displacement ratio (Δ_u / Δ_y). The ductility capacity was found to be greatly affected by the thickness of base steel plate, the fastener number and the fastener spacing. As shown in Figure 15(a), the ductility capacity increases with increasing thickness of base steel plate. This is because the ultimate displacement increases with increasing thickness of base steel plate (see Eq. 19) while the yield displacement remains unchanged according to Eq. (17). Owing to the group effect, the ductility capacity decreases with increasing fastener numbers, see Figure 15(b). Larger fastener spacing can enhance the ductility capacity as shown in Figure 15(c).

5. Bearing resistance of connections

5.1. Predicted maximum bearing resistance - existing specifications

According to ANSI/AISC 360-16 [9], the maximum bearing resistance is given by:

$$F_b = \alpha_{br} d_n t_p f_{pu} \quad (8)$$

where α_{br} is a bearing resistance factor. When deformation at the connected holes is a design consideration, the α_{br} is 2.4. Otherwise, it is 3.0. d_n is the fastener diameter. t_p is the thickness of the thinner steel plate and f_{pu} is the tensile strength of the thinner steel plate.

In the AS 4100 specifications [10], the equation for the bearing resistance is similar to that in ANSI/AISC 360-16 [9] except that the bearing resistance factor is instead represented by one unique value of 3.2.

In EN 1993-1-8 [8], the bearing resistance factor in Eq. (8) is expressed with two other factors to consider the effects of the fastener spacing, edge distance, end

distance and fastener position.

$$\alpha_{br} = k_1 \alpha_b \quad (9)$$

Factor α_b is expressed by:

$$\alpha_{br} = \min \left\{ \alpha_d, \frac{f_{un}}{f_{pu}}, 1 \right\} \quad (10)$$

where $\alpha_d = \frac{e_1}{3d_n}$ for the end fasteners or $\alpha_d = \frac{p_1}{3d_n} - \frac{1}{4}$ for the inner fasteners. e_1 is

the end distance and p_1 is the fastener spacing in the direction of the load transfer.

f_{un} is the fastener strength.

For the edge fasteners, factor k_1 is given by:

$$k_1 = \min \left\{ 2.8 \frac{e_2}{d_n} - 1.7, 1.4 \frac{p_2}{d_n} - 1.7, 2.5 \right\} \quad (11a)$$

For the inner fasteners, factor k_1 is given by:

$$k_1 = \min \left\{ 1.4 \frac{p_2}{d_n} - 1.7, 2.5 \right\} \quad (11b)$$

where e_2 is the edge distance and p_2 is the fastener spacing that is perpendicular to the direction of the load transfer.

The above equations have evolved from those for predicting the maximum bearing resistance of bolt connections due to the lack of specific equations for determining the maximum bearing resistance of connections joined by direct fastening.

In EN 1993-1-3 [22], the equation for determining the maximum bearing resistance of a connection joined by using cartridge fired pins is provided, which is the same as that given in AS 4100. However, this equation which has one unique bearing factor fails to calculate the maximum bearing resistance correctly, which is elaborated as follows.

The results of the measured maximum bearing resistance normalized with that of the predicted maximum bearing resistance based on the above equations evolved from those for predicting the maximum bearing resistance of bolt connections were

summarized in Table 9. The average normalized maximum bearing resistance estimated by using the equations in ANSI/AISC 360-16, AS 4100-1998 (or EN 1993-1-3) and EN 1993-1-8 is 0.87, 0.65 and 0.84, respectively, which indicate that the predicted maximum bearing resistance by these specifications is not conservative, especially that which is predicted by the equation in AS 4100 (or EN 1993-1-3). Furthermore, the discreteness of the normalized maximum bearing resistance with a coefficient of variance (CV) of 0.24 is significant, which can be seen in Figure 16. Hence, a more accurate equation is needed to predict the maximum bearing resistance correctly.

5.2. Proposed expression for predicting maximum bearing resistance

Fasteners can be knurled, which means that a pattern is rolled onto the material. The keying mechanism can be carried out with knurled fasteners. Besides that, one of the unique characteristics is the occurrence of protuberance as shown in Figure 17 when the fasteners are driven into the steel plates. Protuberance can occur on both the connected and base steel plates, but only the protuberance on the connected steel plate is effective which will be verified by samples with different base steel plate thickness. This is subsequently validated. In this section, the effects of these two unique characteristics will be discussed separately.

It can be concluded from the measured maximum bearing resistance in Table 9 that the effects of number, arrangement and spacing of the fasteners are small when compared with the type of fasteners and protuberance. Hence, to facilitate engineers to evaluate the maximum bearing resistance of the connections, these two important effects have been incorporated into Eq. (8) to develop a unified design equation, which is given by:

$$F_b = \psi_{fp} \psi_{fk} \alpha_{br} d_n t_p f_{pu} \quad (12)$$

where ψ_{fp} is a factor for the effect of protuberance and ψ_{fk} is included for the effect of knurling. These three factors are determined in the following sections.

5.2.1. Bearing resistance factor

As stated previously, the format of Eq. (8) was utilized to predict the maximum bearing resistance but the bearing factor was recalibrated. To eliminate the effect of knurling, only the results of the samples connected using the X-S 14 B3 MX fastener were examined. After examining the tested samples that are shown in Figure 18, it can be observed that the fastener is tightly surrounded by the protuberance on the connected steel plate. However, the clamping effect on the protuberance on the base steel plate is eliminated due to the unavoidable fracturing caused by the protuberance. Hence, it is concluded that the protuberance on connected steel plates is effective while that on the base steel plate does not change the maximum bearing resistance. Thus the examined samples should be pre-drilled to eliminate the effect of the protuberance. Forty samples with pre-drilled holes on connected steel plate jointed using the X-S 14 B3 MX fastener are applicable under these requirements and the bearing resistance factors are shown in Figure 19. When the fasteners are driven into the base steel plates with different thicknesses, the fastener head may not tightly contact with the top steel plate, which depends on the thickness of steel plate. When the fastener head tightly contacts with the top steel plate ($t_2 = 2 \text{ mm} - 4 \text{ mm}$), a lower bound value of 1.6 is proposed for the bearing resistance factor. On the other hand, when the fastener head does not tightly contact with the top steel plate ($t_2 = 5 \text{ mm} - 6 \text{ mm}$), the fastening effect is reduced and the bearing resistance factor is smaller. To take into account such effect, a reduction factor of 0.85 should be multiplied by the above lower bound value of 1.6. Owing to the installation requirements, this assembly with fastener head not tightly contacted with the top steel plate is considered inappropriate. Consequently, this type fastener can only join two steel plates with total thickness not over 7 mm.

5.2.2. *Effect of protuberance*

To investigate the effect of protuberance, the tested samples that have pre-drilled holes as well as those without holes drilled into the connected steel plate were analyzed separately and the maximum bearing resistance was normalized with that of the base steel plate with a thickness of 3 mm. For example, the maximum bearing resistance of S275-A-4-4-2(20)-T is normalized by that of S275-A-4-3-2(20)-T. Figure 21(a) shows the normalized maximum bearing resistance of the tested samples with pre-drilled holes on the connected steel plate. The normalized maximum bearing

resistance of the base steel plate with a thickness of 2 mm is close to 0.67 and that of the other base steel plates is around 1.0 by considering the fastening effect mentioned above. This is in accordance with the correct requirements for Eq. (8) and shows that the protuberance on the base steel plate is not effective which is in agreement with Figure 15. Figure 21(b) shows the normalized maximum bearing resistance of the tested samples without pre-drilled holes on the connected steel plate. It can be obviously seen that the normalized maximum bearing resistance for the base steel plates that have a thickness range of 4 mm to 6 mm is over 1.0, which is due to the effect of the protuberance. This indicates that the fastening effect is enhanced by protuberance. Hence, a factor (ψ_{fp}) of 1.35 is used to include the effect of the protuberance.

5.2.3. Effect of knurling on nails

Keying is a specific anchoring mechanism that is only possible with knurled fasteners. To study the effect of this phenomenon, the yield strength of the samples connected by the knurled fastener, X-U 16, was normalized by the maximum bearing resistance of those connected by X-S 14 B3 MX, or the fastener that is not knurled. The diameter effect of these two fasteners was taken into consideration. The normalized maximum bearing resistance was presented in Figure 22. It can be concluded that the maximum bearing resistance can be improved by using knurled fasteners. A factor (ψ_{fk}) of 1.17 was used to quantify the effect of using knurled fasteners. In practice, knurled fasteners can be used to connect steel plates with a total thickness of not more than 10 mm.

5.2.4. Application of proposed equation

All cases (e.g. the effect of protuberance) were included in the proposed equation; see Eq. (12). ψ_{fp} is equal to 1.0 for connections joined with pre-drilled holes on the connected plates while ψ_{fp} is 1.35 for connections without pre-drilled holes on the connected plates. ψ_{fk} is 1.0 and 1.17 for fasteners that are not knurled and knurled fasteners, respectively.

When calibrating the above three factors, only the test data from 80 samples with steel grade of S275 was used. To verify the accuracy of the calibration process, Figure 23(a) shows the normalized maximum bearing resistance which was obtained by dividing the measured maximum bearing resistance with the predicted maximum bearing resistance. The results showed that the average normalized maximum bearing resistance (1.04) is close to 1.0 with a CV of 0.11. This indicates that the calibration process is successful. To validate the effectiveness of Eq.(12), the measured resistance for the samples with steel grade of S355 was normalized by the predicted resistance, see Figure 23(b) and Table 9. The average normalized maximum bearing resistance (0.95) is close to 1.0 with a CV of 0.07. In addition, almost all the normalized maximum bearing resistances fall in the range of 0.8 to 1.2. This indicates that the predicted resistance from Eq.(12) is accurate. Furthermore, when compared with the predicted results by other codified methods as shown in Figure 16, the predicted resistance from Eq.(12) is more accurate with small discreteness.

Behavior of single shear bolted connections at elevated temperature was studied in [7]. They found that deterioration of material properties can be considered as strength deterioration of single shear bolted connections. By adopting such consideration, the following relationship needs to be satisfied with the exclusion of partial safety factors:

$$\phi_b F_b < \phi_{fs} F_{fs} \quad (13)$$

where ϕ_b and ϕ_{fs} are the strength reduction factor or strength residual value of steel plate and the fastener, respectively, under high temperature or post fire, which have been determined in previous sections; F_{fs} is the shear resistance of the fastener under ambient temperature, which can be determined from the recommended expression in EN 1993-1-8 [8], which is given as:

$$F_{fs} = \alpha_{fs} f_{fu} A_f \quad (14)$$

where α_{fs} is the shear capacity factor. f_{fu} represents material tensile strength of fastener. A_f is the nominal cross-sectional area of fastener. α_{fs} is equal to 0.65 and can be calibrated with the samples failed in fastener fracture listed in Table 9. In EN 1993-1-8 [8], this value is 0.6. For conservatism, this value is taken as 0.6 in this study.

6. Proposed simple BRVD curve

The finite element method (FEM) is an effective numerical method that can be used to analyze the behavior of structure systems [25-29]. To accurately simulate the performance of a structure system, the behavior of the connections that are joined by direct fastening should be simulated. In general, there are two ways to do so. One is to construct the real connections through finite element modeling by using solid elements but this method means that the computational cost can be significantly high. This computational costly method should only be used to examine the performance of a single connection. The second method is to replace the real connection by using connected elements which means that the computational efficiency is very much increased. The performance of the real connections is reflected by the plotted BRVD from the experiments as shown in Figure 24. To simulate the connections with various configurations (e.g. number of fasteners), a simple BRVD curve (OABC) was proposed (Figure 24). Three key parameters form the basis of this simple curve. The maximum bearing resistance of the connection has been discussed earlier. Hence, the remaining two parameters, effectiveness stiffness and ultimate displacement, will be discussed in the following section.

6.1. Effective stiffness

The yield displacement can be determined by the maximum bearing resistance and effective stiffness which is defined as follows:

$$K_{ef} = \frac{F_b}{\Delta_y} \quad (15)$$

where K_{ef} denotes the effective stiffness of the connection and Δ_y represents the yield displacement of the connection.

Compared to yield displacement, the physical meaning of effective stiffness is more specific as it is related to the elastic modulus and thickness of the plates and the diameter of the fasteners. Thus, the effective stiffness of the connection should be used to replace yield displacement and it is appropriate to assume the following format for the effective stiffness of the connection:

$$K_{ef} = \frac{\psi_{fn}\psi_{ef}E_s t_p d_n}{l_c} \quad (16)$$

where E_s is the elastic modulus of the plates, ψ_{ef} is the effective stiffness (ES) factor which is calibrated by the test results, ψ_{fn} represents the factor that depends on the number of fasteners (FN), and l_c depicts the characteristic length in which deformation happens.

Owing to the fact that the characteristic length is difficult to define, the effect of this parameter is incorporated into the effective stiffness factor. Hence, the effective stiffness is rewritten as:

$$K_{ef} = \psi_{fn} \psi'_{ef} E_s t_p d_n \quad (17)$$

where ψ'_{ef} is the modified effective stiffness (MES) factor which incorporated the effect of characteristic length.

In total, 11 tested samples were used to determine the MES factor. The results are shown in Figure 25. A value of 0.017 is adopted for the MES factor. The relationship between the FN factor and number of fasteners is shown in Figure 26. It can be seen that the relationship is not exactly linear due to group effect. The average value is used for the FN factor for the number of fasteners in the test, and the FN factors were given by:

$$\psi_{fn} = \begin{cases} 1 & n_n = 1 \\ 1.4 & n_n = 2 \\ 1.9 & n_n = 4 \\ 2.1 & n_n = 6 \end{cases} \quad (18)$$

where n_n represents the number of fasteners.

The FN factor for other quantities of fasteners can be determined by using linear interpolation and extrapolation.

6.2. Ultimate displacement

When the pull-out force exceeds the friction force, the maximum bearing resistance substantially drops to zero. Hence, it is reasonable to assume that the ultimate displacement is set as the displacement when the bearing resistance is reduced to 80% of the maximum bearing resistance. Furthermore, the ultimate displacement can be regarded as the result of the rotation of the fasteners, which can

be determined by:

$$\Delta_u = \frac{t_1 + t_2}{2} \phi_f \quad (19)$$

where ϕ_f is the friction angle or final rotation angle.

Based on the failure modes shown in Figures 13(a) and 12(b) and analysis of the ultimate displacement, it is concluded that the friction angle is influenced by the type of fastener (i.e., whether the fastener is knurled or not knurled). Figure 27 shows that the friction angle of the two types of fasteners is 0.43 rad and 0.75 rad, respectively. It can be concluded that knurled fasteners can increase the deformability of connections.

6.3. Comparison of plotted BRVD

Based on the above work, the BRVD for each connection was plotted into a simple curve. First, the yield strength can be determined by using Eq. (12). Then the yield displacement can be derived by combining Eqs. (12), (15) and (17). Lastly, the ultimate displacement can be obtained with Eq. (19). Some of the predicted and tested BRVDs were plotted into simple curves and compared in Figure 28. It can be observed that the simple curves plotted from the predicted BRVD are in good agreement with the curves plotted from the tested BRVD which proves that the proposed method in this study can be used to predict the behavior of connections.

7. Conclusions

In this paper, the mechanical properties of coupons and fasteners have been examined at high temperatures and after exposure to a fire. Connection samples were tested to investigate the effects of different variables on their bearing resistance, ultimate displacement and effective stiffness. Some of the main conclusions that can be drawn from the work are as follows:

(1) Current specifications, such as EN-1993-1-2 and ANSI/AISC 360-16, can be used to predict the reduction factor of elastic modulus but new reduction factors should be proposed for yield strength probably owing to the different test method in EN-1993-1-2 and this study. Besides that, reduction factor for ultimate strength is missing in current specifications regardless of the test method. Hence, new reduction factors are proposed for yield strength and ultimate strength. Regarding the residual

values for the mechanical properties of mild steel post fire, they experience similar trend in which residual values keep constant to a specific temperature and then decrease with the increase in temperature. To quantify the deterioration in mechanical properties, residual values were recommended. These values are more reasonable than those stated in the current design specifications.

(2) The shear strength of fasteners undergoes a similar trend of decline as that found with the mechanical properties of the coupons at high temperatures and after exposure to a fire. To evaluate the shear strength of fasteners at different temperatures, recommended values were provided based on the test results.

(3) Predicting the maximum bearing resistance with the current specifications is obviously not conservative nor discrete enough. Protuberance and knurled fasteners can enhance the maximum bearing resistance and ultimate displacement can be enhanced with knurled fasteners. By separating the effects of protuberance and knurled fasteners from the bearing factor, modified equations were then formulated which can be used to more accurately predict the maximum bearing resistance.

(4) A simple envelope curve is plotted based on the three key parameters of maximum bearing resistance, effectiveness stiffness and ultimate displacement of the connection samples. The simple curves plotted from the predicted BRVD are in good agreement with the curves plotted from the tested BRVD which proves that the proposed method in this study can be used to predict the behavior of connections.

Acknowledgements

The authors would like to thank the financial support of the RGC Research Impact Fund (R7027-18) entitled “Modular Integrated Construction 2.0+” for Quality and Efficient Tall Residential Buildings through Advanced Structural Engineering, Innovative Building Materials and Smart Project Delivery. Furthermore, the generous support of the direct fastening tools and nails by HILTI Corporation is gratefully acknowledged.

References

[1] Direct fastening technology manual. Hilti Corporation, 2018.

- [2] Lu W, Makelainen P, Outinen J, Ma ZC. Design of screwed steel sheeting connection at ambient and elevated temperatures. *Thin Wall Struct* 2011;49(12): 1526-1533.
- [3] Lu W, Ma ZC, Makelainen P, Outinen J. Behaviour of shear connectors in cold-formed steel sheeting at ambient and elevated temperatures. *Thin Wall Struct* 2012;61: 229-238.
- [4] Lu W, Ma ZC, Makelainen P, Outinen J. Design of shot nailed steel sheeting connection at ambient and elevated temperatures. *Eng Struct* 2013;49: 963-972.
- [5] Yan S, Young B. Screwed connections of thin sheet steels at elevated temperatures—Part I: Steady state tests. *Eng Struct* 2012;35: 234-243.
- [6] Yan S, Young B. Tests of single shear bolted connections of thin sheet steels at elevated temperatures—Part I: Steady state tests. *Thin Wall Struct* 2011;49(10): 1320-1333.
- [7] Cai YC, Young B. Behavior of cold-formed stainless steel single shear bolted connections at elevated temperatures. *Thin Wall Struct* 2014;75: 63-75.
- [8] EN-1993-1-8, Eurocode 3. Design of steel structure. Part 1.8: design of joints. European Committee for Standardization; 2005.
- [9] ANSI/AISC 360-16. Specification for structural steel buildings. American Institute of Steel Construction, Chicago-Illinois;2010.
- [10] AS 4100. Steel Structures. Standards Australia, Sydney;1998.
- [11] ASTM, E 21. Standard test method elevated temperature tension test of metallic materials. American Society for Testing and Materials, West Conshohocken, USA, 2009.
- [12] Li HT, Young B. Residual mechanical properties of high strength steels after exposure to fire. *J Constr Steel Res* 2018;148: 562-571.
- [13] Tan W. Experiments and research of steel material properties at elevated

- temperature. *Indust Constr* 2000;30(10):61-63,67.
- [14] GB50017, Chinese Standard. Code for design of steel structures. Ministry of Construction of the People's Republic of China; 2003.
- [15] EN-1993-1-1. Eurocode 3: Design of steel structures. Part 1.1: General rules and rules for buildings. European Committee for Standardization; 2005.
- [16] EN-1993-1-2. Eurocode 3: Design of steel structures, Part 1.2: General rules-structure fire design. European Committee for Standardization;2005.
- [17] BS5950. Structure use of steel work in building, Part 8: Code of practice for fire resistant design. British Standard Institute, London, UK,2000.
- [18] Ding FX, Yu ZW, Wen HL. Experimental research on mechanical properties of Q235 steel after high temperature treatment. *J Build Master* 2006;9(2):245-249.
- [19] Zhang YJ, Zhu Y, Zhao S, Hu KX. Experimental research on mechanical properties of steel cooled in different modes after high temperature treatment. *Sturct Eng* 2009;25(5):104-109.
- [20] Chen JF, Chao PZ. Experimental investigation into mechanical properties of steel post high temperatures. *J PLA Uni Sci Technol Nat Sci Ed* 2010;11(3):328-333.
- [21] Outinen J, Makelainen P. Mechanical properties of structural steel at elevated temperatures and after cooling down. *Fire Mater* 2004;28:237-251.
- [22] EN-1993-1-3, Eurocode 3. Design of steel structure. Part 1.3: supplementary rules for cold-formed members and sheeting. European Committee for Standardization; 2006.
- [23] Qiang X, Bijlaard F, Kolstein H. Post-fire mechanical properties of high strength structural steels S460 and S690. *Eng Struct* 2012;35:1-10.
- [24] Qiang X, Bijlaard F, Kolstein H. Post-fire performance of very high strength steel S960. *J Constr Steel Res* 2013;80:235-242.
- [25] Gödrich L, Wald F, Kabeláč J, Kuříková M. Design finite element model of a

- bolted T-stub connection component. *J Constr Steel Res* 2019;157:198-206.
- [26] Lingfei K, Heling J, Ghasemi AH, Yan L. Condensation modeling of the bolted joint structure with the effect of nonlinear dynamics. *J Sound Vib* 2019; 442:657-676.
- [27] Tahir MM, Mohammadhosseini H, Ngian SP, Effendi MK. I-beam to square hollow column blind bolted moment connection: Experimental and numerical study. *J Constr Steel Res* 2018;148:383-398.
- [28] Brunesi E, Nascimbene R, Rassati GA. Response of partially-restrained bolted beam-to-column connections under cyclic loads. *J Constr Steel Res* 2014;97:24-38
- [29] Gray PJ, McCarthy CT. An analytical model for the prediction of through-thickness stiffness in tension-loaded composite bolted joints. *Compos Struct* 2012; 94(8): 2450-2459.

Notations

Rd_E	reduction factor of elastic modulus of steel under high temperatures
Rd_y	reduction factor of yield strength of steel under high temperatures
Rd_u	reduction factor of ultimate strength of steel under high temperatures
Rs_E	reduction factor of elastic modulus of steel after exposure to fire
Rs_y	reduction factor of yield strength of steel after exposure to fire
Rs_u	reduction factor of ultimate strength of steel after exposure to fire
T	temperature
Rd_f	reduction strength factor of fastener
Rs_f	residual strength factor of fastener
d_0	diameter of fastener hole
F_b	bearing resistance
α_{br}	bearing resistance factor
d_n	diameter of fastener
t_p	thickness of thinner steel plate
f_{pu}	tensile strength of thinner steel plate
e_1	end distance
p_1	fastener spacing in direction of load transfer
f_{un}	fastener strength
e_2	edge distance
p_2	fastener spacing perpendicular to direction of load transfer
ψ_{fp}	protuberance factor
ψ_{fk}	keying factor
K_{ef}	effective stiffness of connection
l_c	the character length
ψ_{ef}	effective stiffness factor
ψ'_{ef}	Modified effective stiffness factor
ψ_{fn}	factor that depends on number of fasteners
n_n	number of fasteners
n	number of coupons
ϕ_f	friction angle
Δ_y	yield displacement of connection
Δ_u	ultimate displacement of connection
t_1	thickness of connected steel plates
t_2	thickness of base steel plate
F_{fs}	shear resistance of fastener under ambient temperature
$F_{fs,ht}$	shear resistance of fastener under high temperature

$F_{fs,pt}$	shear resistance of fastener post fire
α_{fs}	shear capacity factor
f_{fu}	material tensile strength of fastener
A_f	nominal cross-sectional area of fastener
ϕ_b	reduction factor or residual factor of steel
ϕ_{fs}	reduction factor or residual factor of the fastener
E_s	elastic modulus of steel material under ambient temperature
f_{py}	yield strength of steel material under ambient temperature
f_{pu}	ultimate strength of steel material under ambient temperature
$E_{s,ht}$	elastic modulus of steel material under high temperature
$f_{py,ht}$	yield strength of steel material under high temperature
$f_{pu,ht}$	ultimate strength of steel material under high temperature
$E_{s,pt}$	elastic modulus of steel material post fire
$f_{py,pt}$	yield strength of steel material post fire
$f_{pu,pt}$	ultimate strength of steel material post fire

Table 1 Steel material properties in ambient temperature

Steel grade	E_s (GPa)	f_{py} (MPa)	f_{pu} (MPa)	n
S275	203	317	460	6
S355	210	439	547	5

where E_s is the elastic modulus of steel material under ambient temperature; f_{py} is the yield strength of steel material under ambient temperature; f_{pu} is the ultimate strength of steel material under ambient temperature and n denotes the number of coupons for test.

Table 2 Summary of test plan for steel materials

Types of the tests	Material grade	The temperature (°C)
Tests under high temperatures	S275	200,300,400,500,600,700
	S355	250,300,450,500,650,700
Tests post fire	S275	300,500,600,700,800,900
	S355	200,400,550,650,750,850

Table 3 Steel reduction factors under high temperatures

S275	Nominal temperature	20	200	300	400	500	600	700
	$E_{s,ht}/E_s$	1.0	0.85	0.75	0.62	0.49	0.3	0.29
	$f_{py,ht}/f_{py}$	1.0	1.05	0.9	0.85	0.6	0.33	0.20
	$f_{pu,ht}/f_{pu}$	1.0	1.09	1.13	0.76	0.59	0.24	0.15
S355	Nominal temperature	20	250	300	450	500	650	700
	$E_{s,ht}/E_s$	1.0	0.84	0.91	0.71	0.62	0.43	0.24
	$f_{py,ht}/f_{py}$	1.0	0.88	0.84	0.62	0.57	0.33	0.17
	$f_{pu,ht}/f_{pu}$	1.0	1.0	1.02	0.68	0.51	0.26	0.14

where $E_{s,ht}$ is the elastic modulus of steel material under high temperature; $f_{py,ht}$ is the yield strength of steel material under high temperature; $f_{pu,ht}$ is the ultimate strength of steel material under high temperature. Unit of temperature is degree Celsius (°C).

Table 4 Steel reduction factors under high temperatures based on [13]

Q235 [13]	Nominal temperature	20	200	250	300	350	400	450	500	550	600
	$E_{s,ht}/E_s$	1.0	0.95	0.93	0.88	0.88	0.81	0.73	0.61	0.41	0.15
	$f_{py,ht}/f_{py}$	1.0	0.82	0.80	0.61	0.53	0.49	0.49	0.39	0.23	0.21
	$f_{pu,ht}/f_{pu}$	1.0	1.1	1.1	1.0	0.84	0.66	0.56	0.43	0.31	0.22

Note: unit of temperature is degree Celsius ($^{\circ}\text{C}$).

Table 5 Steel residual factors post fire

S275	Nominal temperature	20	300	500	600	700	800	900
	$E_{s,pt}/E_s$	1.0	1.02	0.96	0.97	0.96	0.97	0.94
	$f_{py,pt}/f_{py}$	1.0	1.03	0.99	0.95	0.93	0.91	0.85
	$f_{pu,pt}/f_{pu}$	1.0	1.01	1.0	0.96	0.92	0.9	0.91
S355	Nominal temperature	20	200	400	550	650	750	850
	$E_{s,pt}/E_s$	1.0	0.98	0.96	1.0	0.97	0.95	0.92
	$f_{py,pt}/f_{py}$	1.0	1.01	0.95	0.96	0.93	0.9	0.97
	$f_{pu,pt}/f_{pu}$	1.0	1.03	1.0	0.98	0.96	0.89	0.89

where $E_{s,pt}$ is the elastic modulus of steel material post fire; $f_{py,pt}$ is the yield strength of steel material post fire; $f_{pu,pt}$ is the ultimate strength of steel material post fire. Unit of temperature is degree Celsius ($^{\circ}\text{C}$).

Table 6 Steel residual factors post fire based on [18-21]

Q235 [19]	Nominal temperature	20	200	400	600	800	-	-
	$E_{s,pf}/E_s$	1.0	0.97	0.97	0.99	1.0	-	-
	$f_{py,pf}/f_{py}$	1.0	0.96	0.99	0.99	1.06	-	-
	$f_{pu,pf}/f_{pu}$	1.0	0.99	1.0	1.0	1.05	-	-
Q235 [20]	Nominal temperature	20	400	500	600	700	800	900
	$E_{s,pf}/E_s$	1.0	0.98	0.95	1.0	0.95	0.95	0.94
	$f_{py,pf}/f_{py}$	1.0	0.96	0.94	0.93	0.90	0.86	0.83
	$f_{pu,pf}/f_{pu}$	1.0	1.0	0.99	0.96	0.93	0.92	0.92
Q235 [18]	Nominal temperature	20	200	400	500	700	1000	-
	$E_{s,pf}/E_s$	1.0	0.98	0.96	0.99	0.99	1.0	-
	$f_{py,pf}/f_{py}$	1.0	1.0	1.07	0.95	0.93	0.42	-
	$f_{pu,pf}/f_{pu}$	1.0	1.03	0.94	0.91	0.88	0.54	-
S355 [21]	Nominal temperature	20	330	500	530	610	670	-
	$E_{s,pf}/E_s$	1.0	1.03	1.02	1.0	0.96	-	-
	$f_{py,pf}/f_{py}$	1.0	1.0	-	0.98	-	0.98	-
	$f_{pu,pf}/f_{pu}$	1.0	-	-	-	-	-	-

Note: dash '-' means that not applicable and unit of temperature is degree Celsius (°C).

Table 7 Fastener reduction strength factors under high temperatures

X-S 14 B3 MX	Nominal temperature	20	150	250	350	410	500	570	660
	$F_{fs,ht}/ F_{fs}$	1.0	1.0	0.85	0.6	0.38	0.26	0.15	0.06
X-U 16	Nominal temperature	20	300	400	500	600	700	-	-
	$F_{fs,ht}/ F_{fs}$	1.0	0.7	0.46	0.26	0.13	0.05	-	-
Recommendations [1]	Nominal temperature	20	200	300	350	400	500	600	700
	$F_{fs,ht}/ F_{fs}$	1.0	1.0	0.82	0.62	0.45	0.24	0.15	0.12

where $F_{fs,ht}$ is the shear resistance of fastener under high temperature and F_{fs} is the shear resistance of fastener under ambient temperature. Unit of temperature is degree Celsius ($^{\circ}\text{C}$).

Table 8 Fastener residual strength factors post fire

X-S 14 B3 MX	Nominal temperature	20	300	400	500	600	700	800
	$F_{fs,pt}/ F_{fs}$	1.0	0.8	0.78	0.57	0.48	0.40	0.46
X-U 16	Nominal temperature	20	300	400	500	600	700	800
	$F_{fs,pt}/ F_{fs}$	1.0	0.97	0.8	0.6	0.54	0.41	0.52

where $F_{fs,pt}$ is the shear resistance of fastener post fire. Unit of temperature is degree Celsius ($^{\circ}\text{C}$).

Table 9 Comparison of predicted bearing resistance

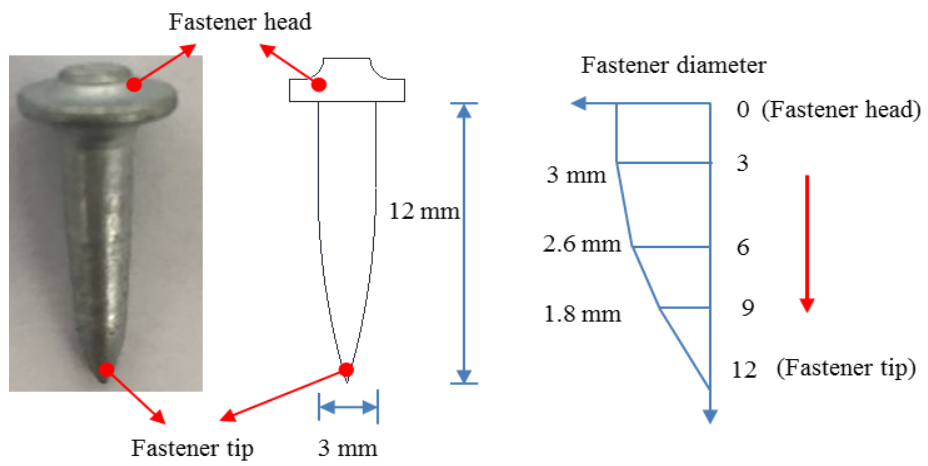
Sample	$F_{b,test}/kN$	$F_{b,test}/F_{b,AISC360}$	$F_{b,test}/F_{b,AS4100}$ Or $F_{b,test}/F_{b,EN1993-1-3}$	$F_{b,test}/F_{b,EN1993-1-8}$	$F_{b,test}/F_{b,proposed}$	Failure mode
S275-A-3-2-1	4.826	0.74	0.56	0.71	1.12	B
S275-A-3-2-2(20)-T	11.061	0.85	0.64	0.82	1.28	B
S275-A-3-2-2(20)-L	11.11	0.86	0.64	0.82	1.29	B
S275-A-3-2-4(20)	19.816	0.79	0.59	0.76	1.18	B
S275-A-3-2-4(30)	20.668	0.82	0.62	0.79	1.23	B
S275-A-3-2-4(40)	23.986	0.95	0.72	0.92	1.43	B
S275-A-3-2-6(20)-T	27.397	0.73	0.55	0.70	1.09	B
S275-A-3-2-6(20)-L	29.726	0.79	0.59	0.76	1.18	B
S275-A-4-2-1	8.208	0.95	0.71	0.91	0.90	B
S275-A-4-2-2(20)-T	15.015	0.87	0.65	0.83	0.83	B
S275-A-4-2-2(20)-L	11.297	0.65	0.49	0.63	0.62	B
S275-A-4-2-4(30)	19.522	0.56	0.42	0.54	0.54	B
S275-A-4-2-4(20)	19.745	0.57	0.43	0.55	0.54	B
S275-A-4-2-4(40)	24.834	0.72	0.54	0.69	0.68	B
S275-A-4-2-6(20)-T	17.71	0.34	0.26	0.33	0.32	B
S275-A-4-2-6(20)-L	19.633	0.38	0.28	0.36	0.36	B
S275-A-3-3-1	7.313	0.75	0.56	0.72	1.13	B
S275-A-3-3-2(20)-T	14.125	0.73	0.54	0.70	1.09	B
S275-A-3-3-2(20)-L	14.385	0.74	0.55	0.71	1.11	B
S275-A-3-3-4(20)	26.772	0.69	0.52	0.66	1.03	B
S275-A-3-3-4(30)	28.109	0.72	0.54	0.69	1.08	B
S275-A-3-3-4(40)	29.001	0.75	0.56	0.72	1.12	B
S275-A-3-3-6(20)-T	41.709	0.72	0.54	0.69	1.07	B
S275-A-3-3-6(20)-L	39.323	0.67	0.51	0.65	1.01	B
S275-A-4-3-1	11.24	0.87	0.65	0.83	1.11	B
S275-A-4-3-2(20)-T	21.687	0.84	0.63	0.80	1.07	B
S275-A-4-3-2(20)-L	21.771	0.84	0.63	0.81	1.08	B
S275-A-4-3-4(30)	28.913	0.56	0.42	0.54	0.53	B
S275-A-4-3-4(20)	25.704	0.50	0.37	0.48	0.47	B
S275-A-4-3-4(40)	45.802	0.88	0.66	0.85	1.13	B
S275-A-4-3-6(20)-T	60.462	0.78	0.58	0.75	1.00	B
S275-A-4-3-6(20)-L	59.228	0.76	0.57	0.73	0.98	B

S275-A-3-4-1	7.098	0.73	0.55	0.70	1.10	B
S275-A-3-4-2(20)-T	14.302	0.74	0.55	0.71	1.10	B
S275-A-3-4-2(20)-L	14.319	0.74	0.55	0.71	1.10	B
S275-A-3-4-4(20)	29.61	0.76	0.57	0.73	1.14	B
S275-A-3-4-4(30)	26.462	0.68	0.51	0.65	1.02	B
S275-A-3-4-4(40)	29.028	0.75	0.56	0.72	1.12	B
S275-A-3-4-6(20)-T	44.735	0.77	0.58	0.74	1.15	B
S275-A-3-4-6(20)-L	45.054	0.77	0.58	0.74	1.16	B
S275-A-4-4-1	16.054	1.24	0.93	1.19	1.18	B
S275-A-4-4-2(20)-T	26.943	1.04	0.78	1.00	0.99	B
S275-A-4-4-2(20)-L	29.487	1.14	0.85	1.09	1.08	B
S275-A-4-4-4(30)	56.885	1.10	0.82	1.05	1.04	B
S275-A-4-4-4(20)	51.155	0.99	0.74	0.95	0.94	B
S275-A-4-4-4(40)	61.143	1.18	0.88	1.13	1.12	B
S275-A-4-4-6(20)-T	80.161	1.03	0.77	0.99	0.98	B
S275-A-4-4-6(20)-L	83.851	1.08	0.81	1.04	1.02	B
S275-A-3-5-1	6.676	0.69	0.52	0.66	1.03	B
S275-A-3-5-2(20)-T	12.443	0.64	0.48	0.61	0.96	B
S275-A-3-5-2(20)-L	13.108	0.67	0.51	0.65	1.01	B
S275-A-3-5-4(20)	25.1	0.65	0.48	0.62	0.97	B
S275-A-3-5-4(30)	23.517	0.60	0.45	0.58	0.91	B
S275-A-3-5-4(40)	24.463	0.63	0.47	0.60	0.94	B
S275-A-3-5-6(20)-T	36.297	0.62	0.47	0.60	0.93	B
S275-A-3-5-6(20)-L	37	0.63	0.48	0.61	0.95	B
S275-A-4-5-1	16.714	1.29	0.97	1.24	1.22	B
S275-A-4-5-2(20)-T	30.732	1.19	0.89	1.14	1.13	B
S275-A-4-5-2(20)-L	33.007	1.27	0.96	1.22	1.21	B
S275-A-4-5-4(30)	62.431	1.20	0.90	1.16	1.14	B
S275-A-4-5-4(20)	61.252	1.18	0.89	1.13	1.12	B
S275-A-4-5-4(40)	66.149	1.28	0.96	1.22	1.21	B
S275-A-4-5-6(20)-T	86.402	1.11	0.83	1.07	1.05	B
S275-A-4-5-6(20)-L	86.694	1.11	0.84	1.07	1.06	B
S275-A-3-6-1	6.142	0.63	0.47	0.61	0.95	B
S275-A-3-6-2(20)-T	11.839	0.61	0.46	0.58	0.91	B
S275-A-3-6-2(20)-L	11.457	0.59	0.44	0.57	0.88	B
S275-A-3-6-4(20)	22.831	0.59	0.44	0.56	0.88	B
S275-A-3-6-4(30)	23.79	0.61	0.46	0.59	0.92	B

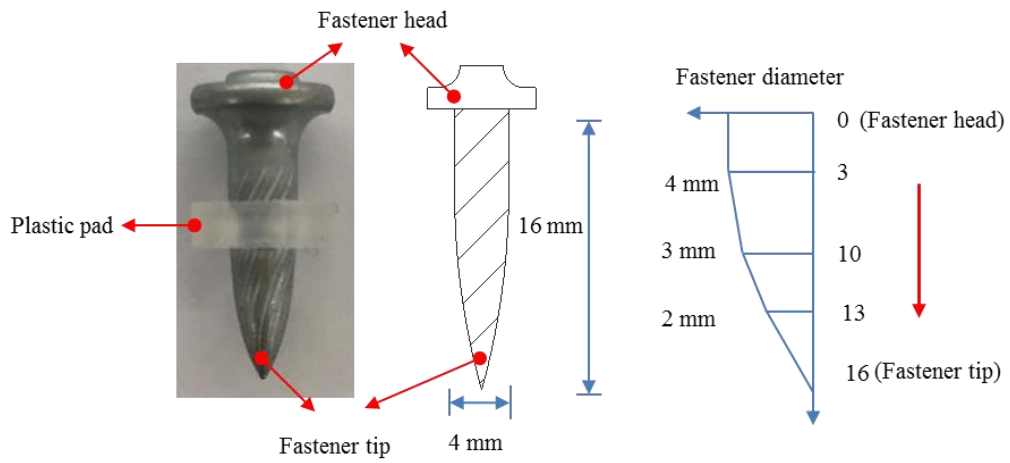
S275-A-3-6-4(40)	25.322	0.65	0.49	0.63	0.98	B
S275-A-3-6-6(20)-T	34.874	0.60	0.45	0.57	0.90	B
S275-A-3-6-6(20)-L	35.83	0.61	0.46	0.59	0.92	B
S275-A-4-6-1	15.888	1.23	0.92	1.18	1.16	B
S275-A-4-6-2(20)-T	32.129	1.24	0.93	1.19	1.18	B
S275-A-4-6-2(20)-L	31.758	1.23	0.92	1.18	1.16	B
S275-A-4-6-4(30)	61.805	1.19	0.89	1.14	1.13	B
S275-A-4-6-4(20)	62.253	1.20	0.90	1.15	1.14	B
S275-A-4-6-4(40)	62.917	1.21	0.91	1.17	1.15	B
S275-A-4-6-6(20)-T	90.349	1.16	0.87	1.12	1.10	B
S275-A-4-6-6(20)-L	89.924	1.16	0.87	1.11	1.10	B
S355-A-4-3-1	13.862	0.88	0.66	0.84	1.12	B
S355-A-4-3-2(20)-T	24.751	0.78	0.59	0.75	1.00	B
S355-A-4-3-2(20)-L	24.943	0.79	0.59	0.76	1.01	B
S355-A-4-3-4(30)	46.249	0.73	0.55	0.70	0.94	B
S355-A-4-3-4(20)	32.219	0.51	0.38	0.49	0.65	B
S355-A-4-3-4(40)	49.53	0.78	0.59	0.75	1.00	B
S355-A-4-3-6(20)-T	70.666	0.74	0.56	0.71	0.95	B
S355-A-4-3-6(20)-L	69.888	0.74	0.55	0.71	0.94	B
S355-A-4-4-1	15.752	0.99	0.75	0.95	0.94	B
S355-A-4-4-2(20)-T	30.006	0.95	0.71	0.91	0.90	B
S355-A-4-4-2(20)-L	33.112	1.05	0.78	1.00	0.99	B
S355-A-4-4-4(30)	61.325	0.97	0.73	0.93	0.92	B
S355-A-4-4-4(20)	57.3	0.90	0.68	0.87	0.86	B
S355-A-4-4-4(40)	65.685	1.04	0.78	1.00	0.98	B
S355-A-4-4-6(20)-T	90.675	0.95	0.72	0.92	0.91	B
S355-A-4-4-6(20)-L	84.011	0.88	0.66	0.85	0.84	B
S355-A-4-5-1	17.19	-	-	-	-	NF
S355-A-4-5-2(20)-L	34.73	-	-	-	-	NF
S355-A-4-6-1	17.28	-	-	-	-	NF
S355-A-4-6-2(20)-L	35.52	-	-	-	-	NF
Average	-	0.87	0.65	0.84	1.04	-
Coefficient of variance	-	0.24	0.24	0.24	0.11	-

Notes: ‘B’ denotes bearing failure and ‘NF’ represents fastener shear fracture. Dashed line ‘-’ means not applicable. Results in bold are bad points and removed from data analysis. $F_{b, test}$ is measured bearing resistance. $F_{b, AISC360}$ is predicted bearing resistance

by using ANSI/AISC 360-16. $F_{b,AS4100}$ and $F_{b,EN1993-1-3}$ represent predicted bearing resistance by using AS 4100 and EN 1993-1-3, respectively. $F_{b,EN1993-1-8}$ and $F_{b,proposed}$ are bearing resistance predicted by EN 1993-1-8 and the proposed method.



(a)



(b)

Fig.1. Details of fasteners: (a) X-S 14 B3 MX and (b) X-U 16



Fig.2. Test setup

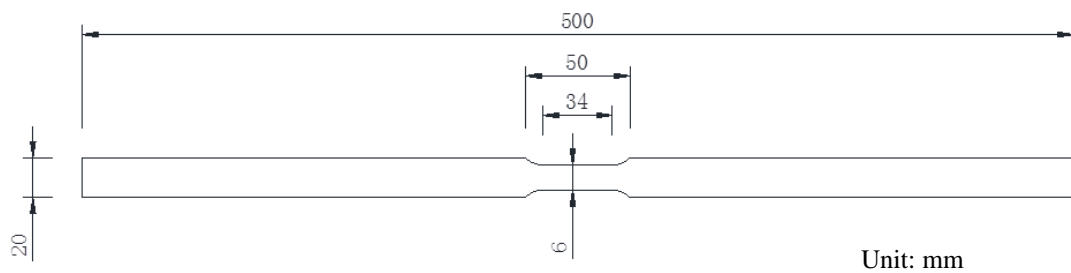


Fig.3. Coupon dimensions

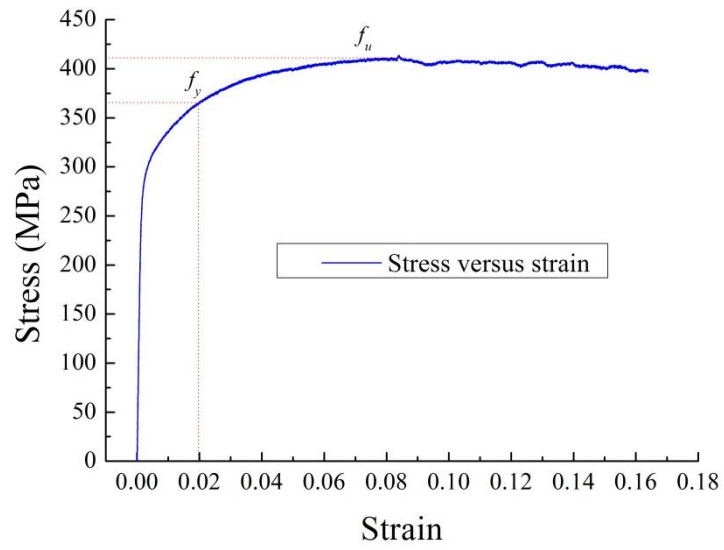
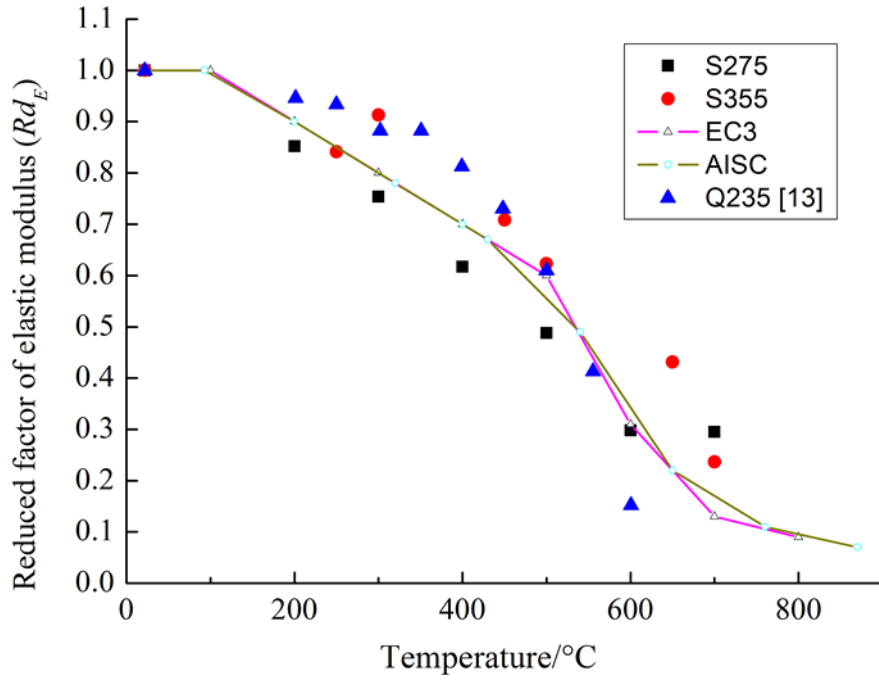
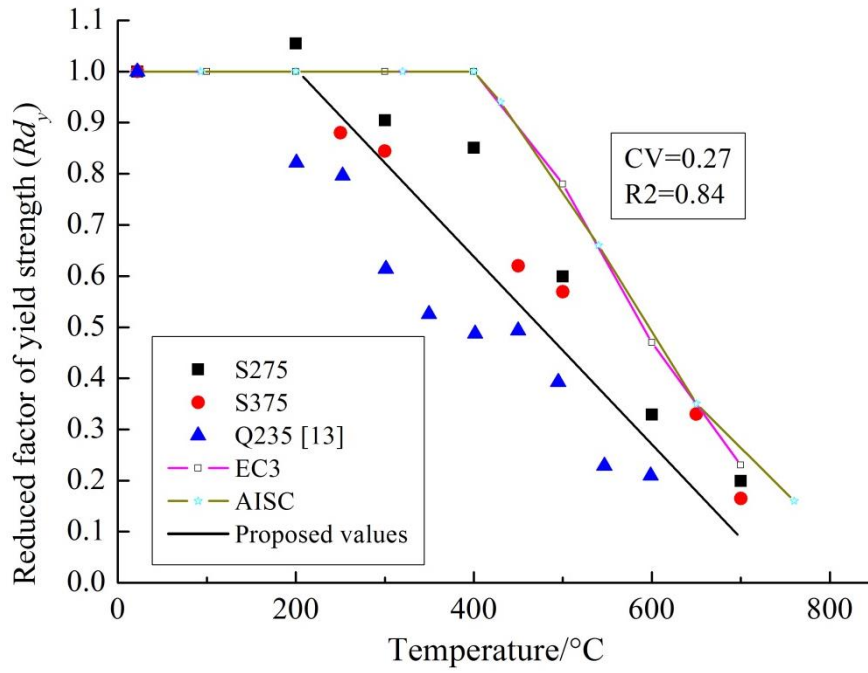


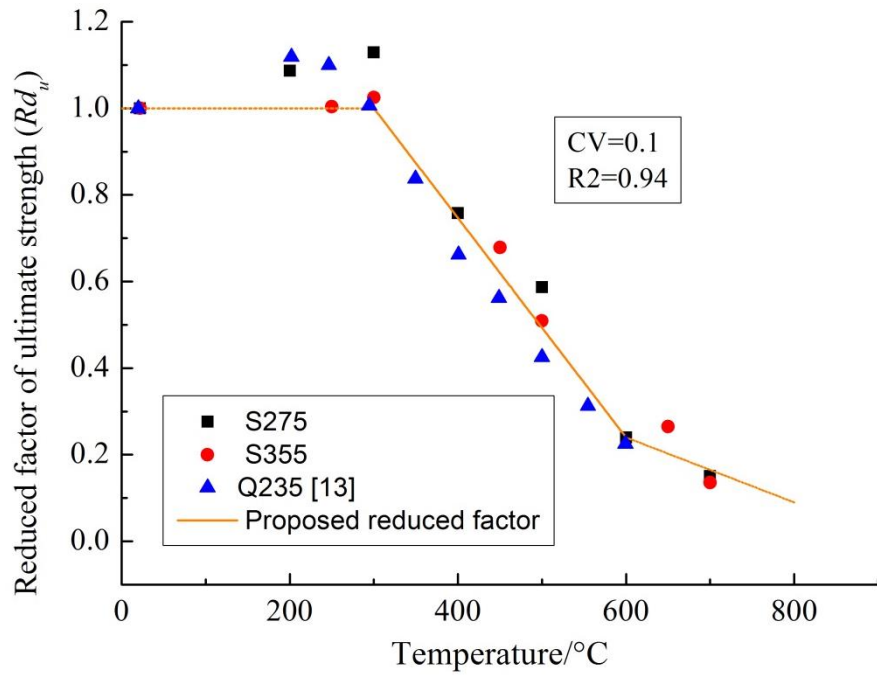
Fig.4. Yield strength at the 2% strain



(a)

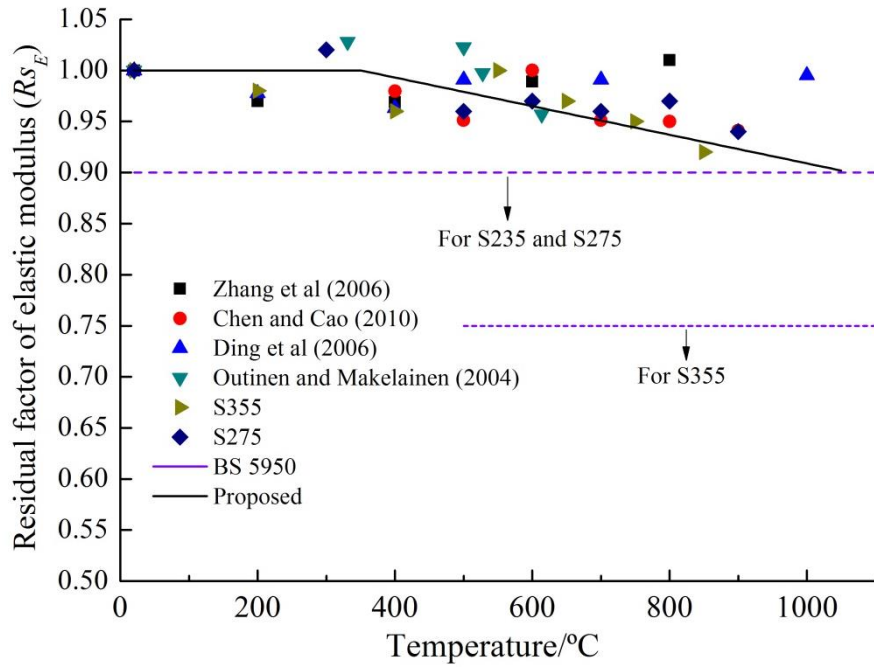


(b)

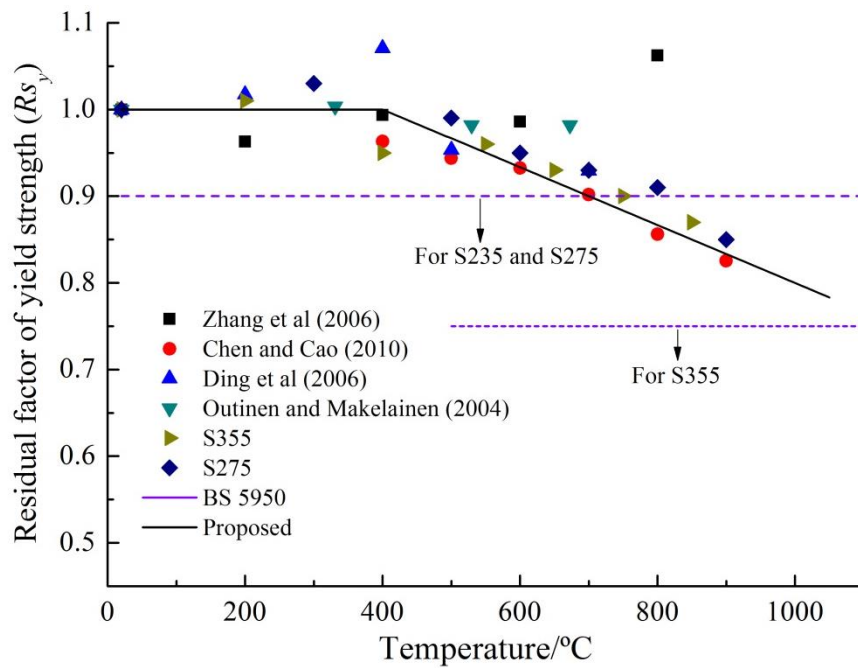


(c)

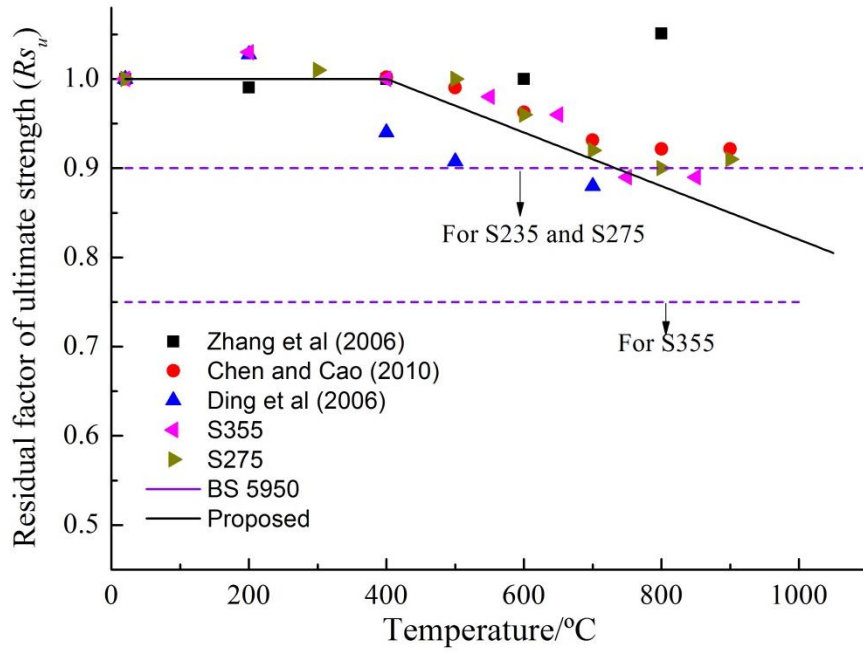
Fig.5. Reduction factors of steel properties at high temperatures: (a) elastic modulus, (b) yield strength and (c) ultimate strength



(a)



(b)



(c)

Fig.6. Residual factors of steel properties post fire: (a) elastic modulus, (b) yield strength and (c) ultimate strength

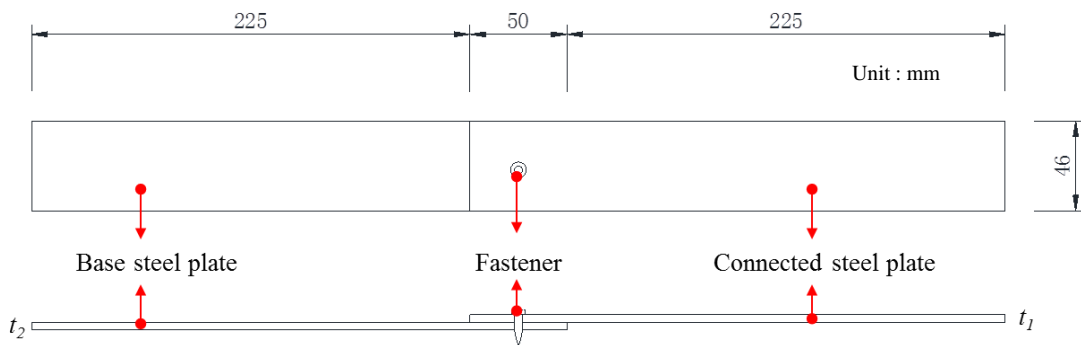


Fig.7. Sample dimensions for testing at high temperatures

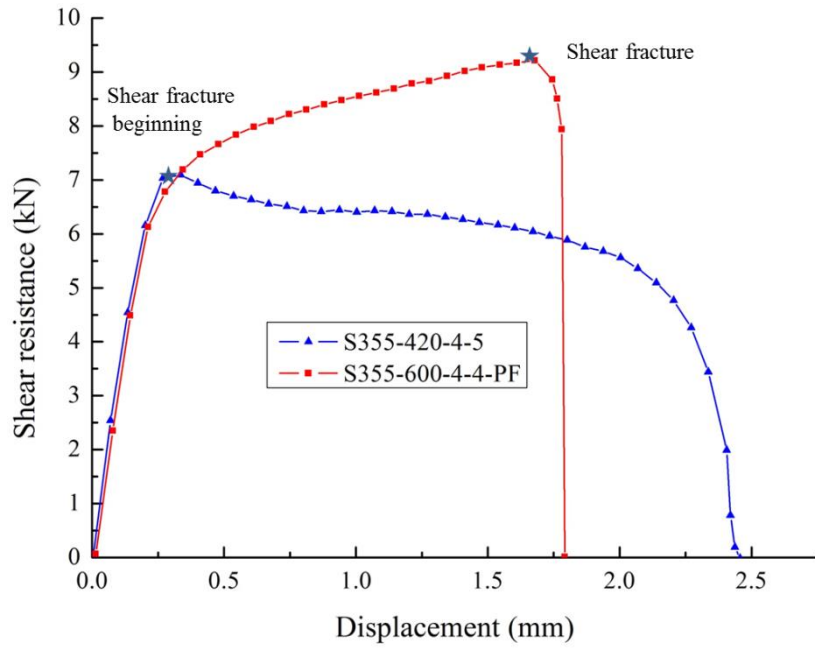


Fig.8. Shear resistance versus displacement curve of fasteners

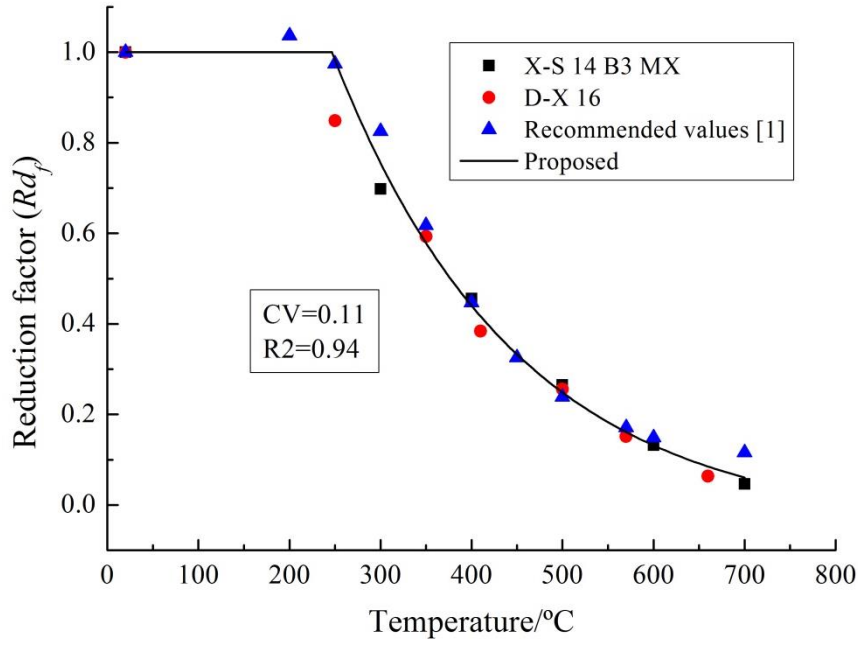


Fig.9. Reduction strength factor of fasteners at high temperatures

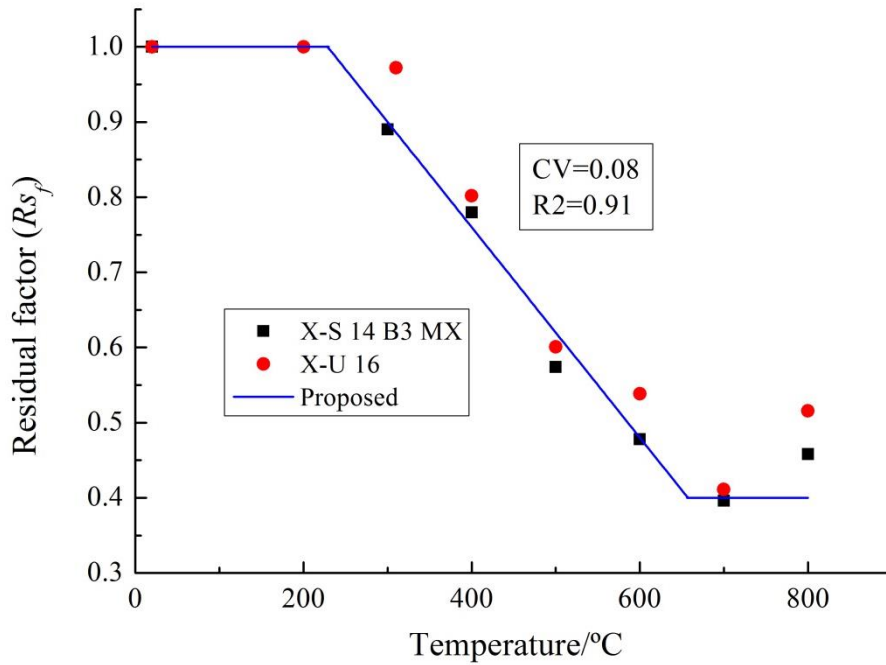


Fig.10. Residual strength factor of fasteners post fire

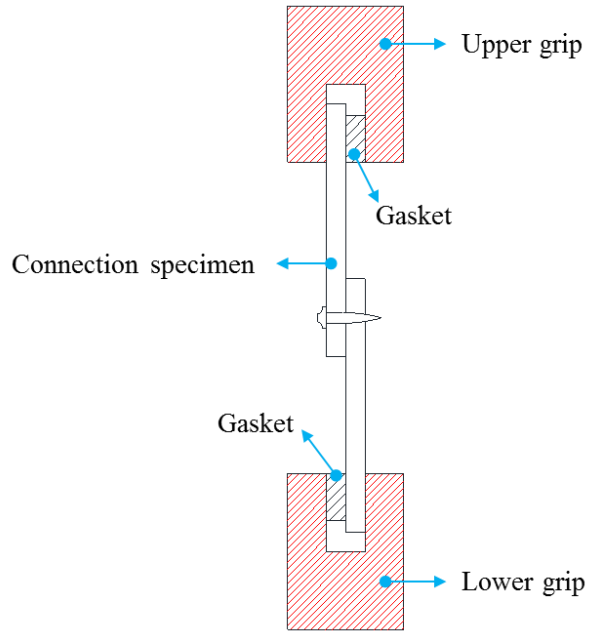


Fig.11. Assembly diagram of connection sample

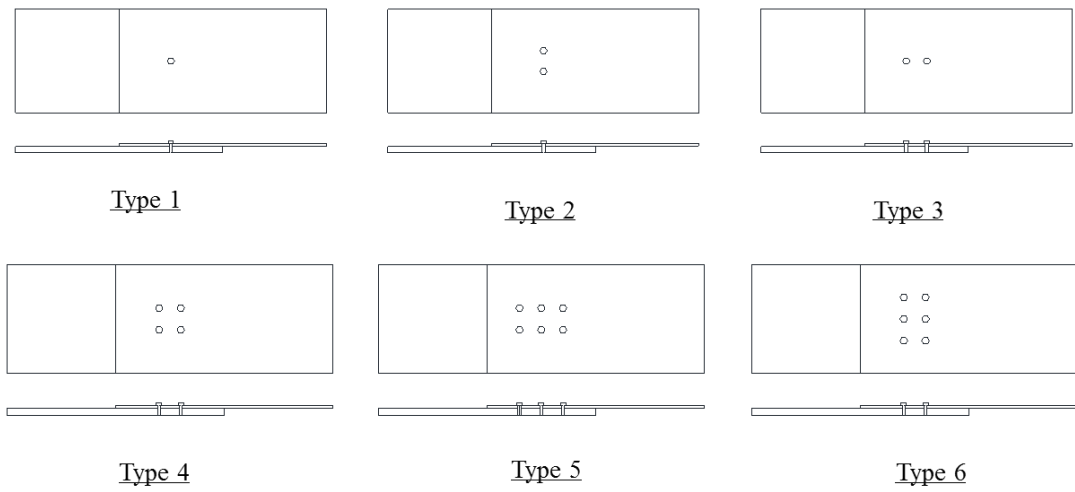
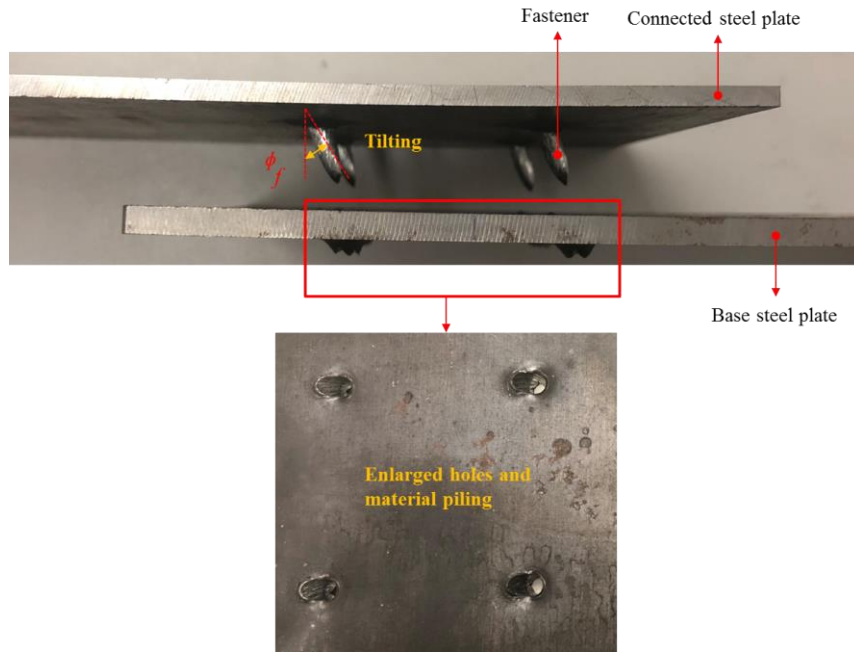
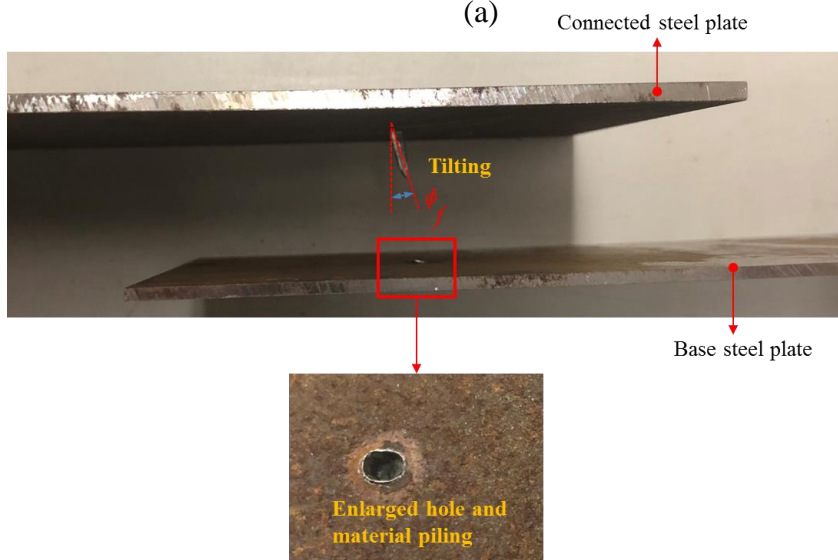


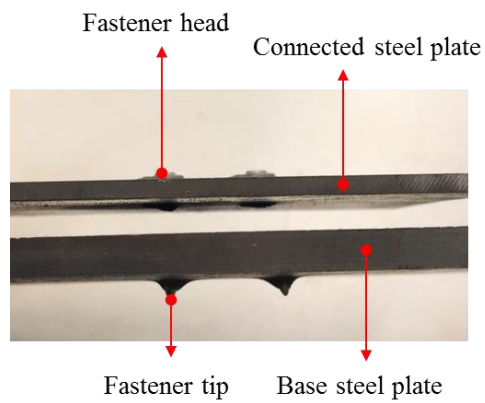
Fig.12. Types of connection samples



(a)



(b)



(c)

Fig.13. Failure modes (a) S275-A-4-4-4(30), (b) S275-A-3-2-1 and S355-A-4-6-2-L

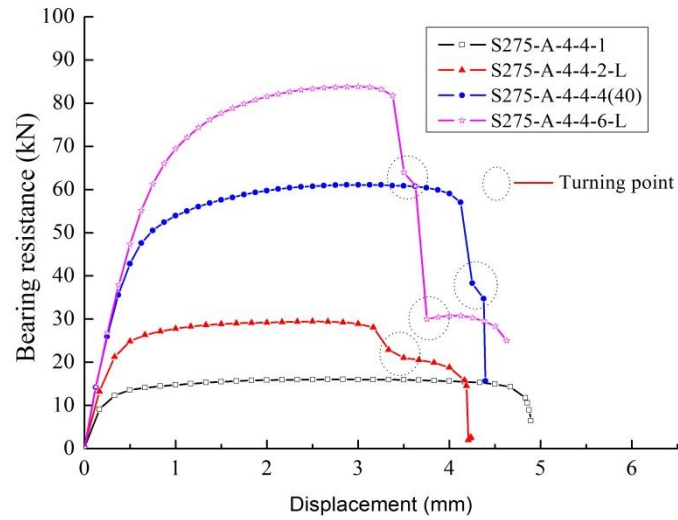


Fig.14. Bearing resistance versus displacement

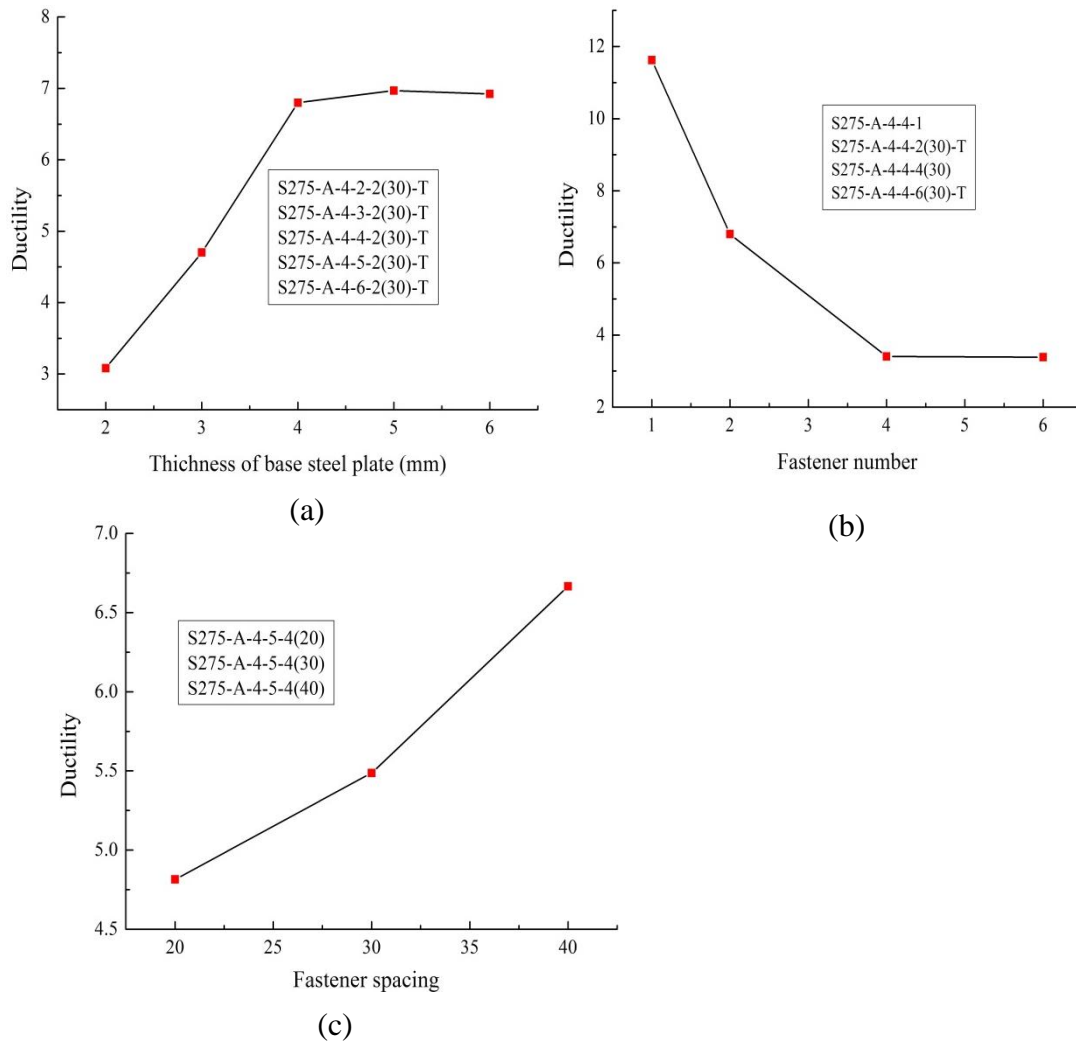


Fig.15. Ductility behavior (a) effect of thickness of base steel plate (b) effect of fastener number and (c) effect of fastener spacing

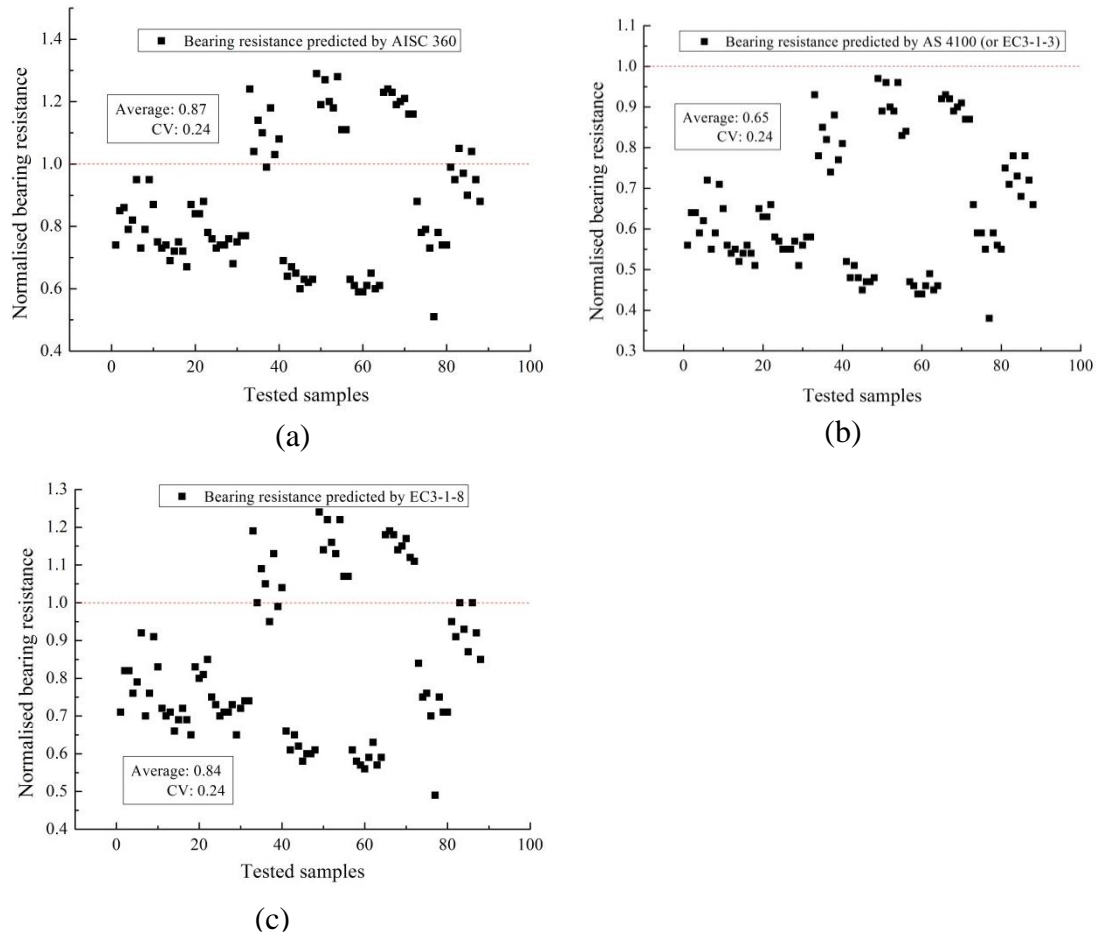


Fig.16. Comparison of predicted bearing resistance (a) yield strength predicted by AISC 360, (b) yield strength predicted by AS 4100 (or EN 1993-1-3) and (c) yield strength predicted by EN 1993-1-8

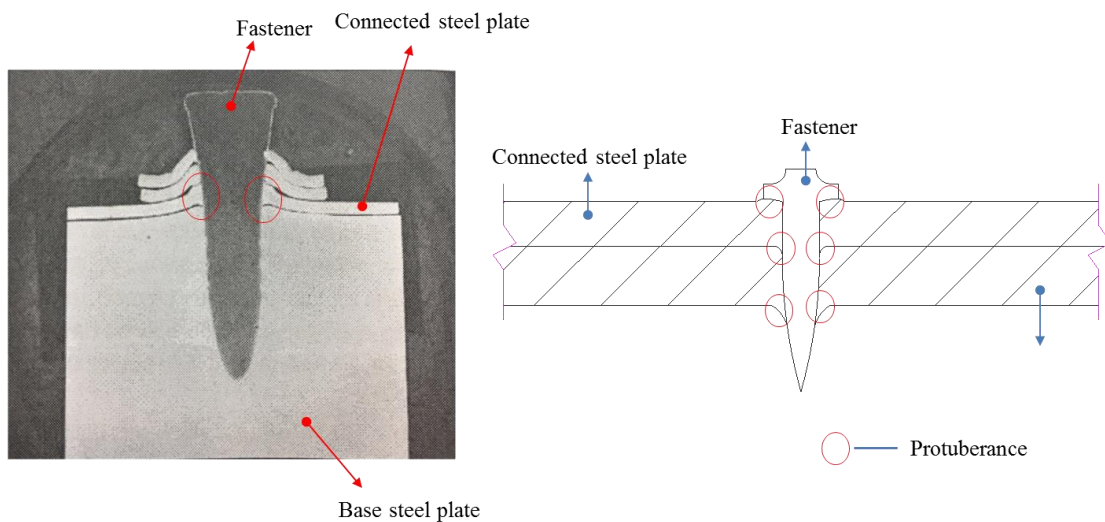


Fig. 17. Schematics of protuberance

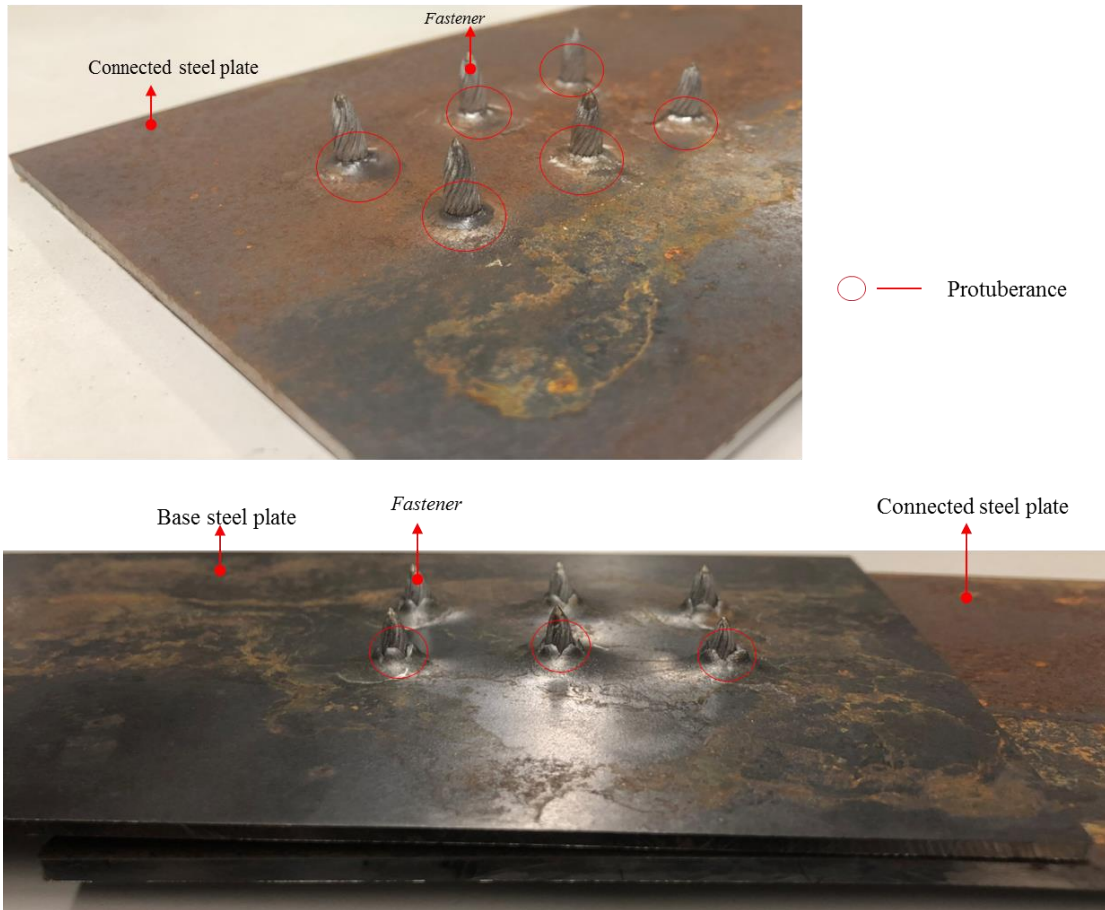


Fig.18. Photos of protuberance

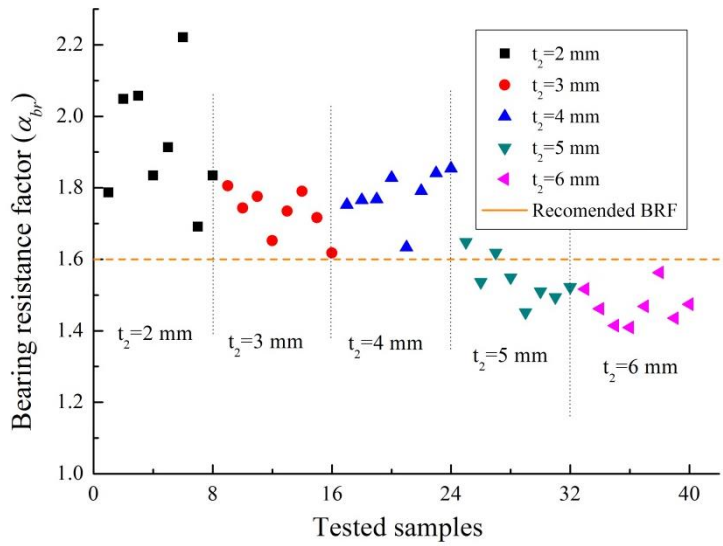


Fig.19. Bearing resistance factor

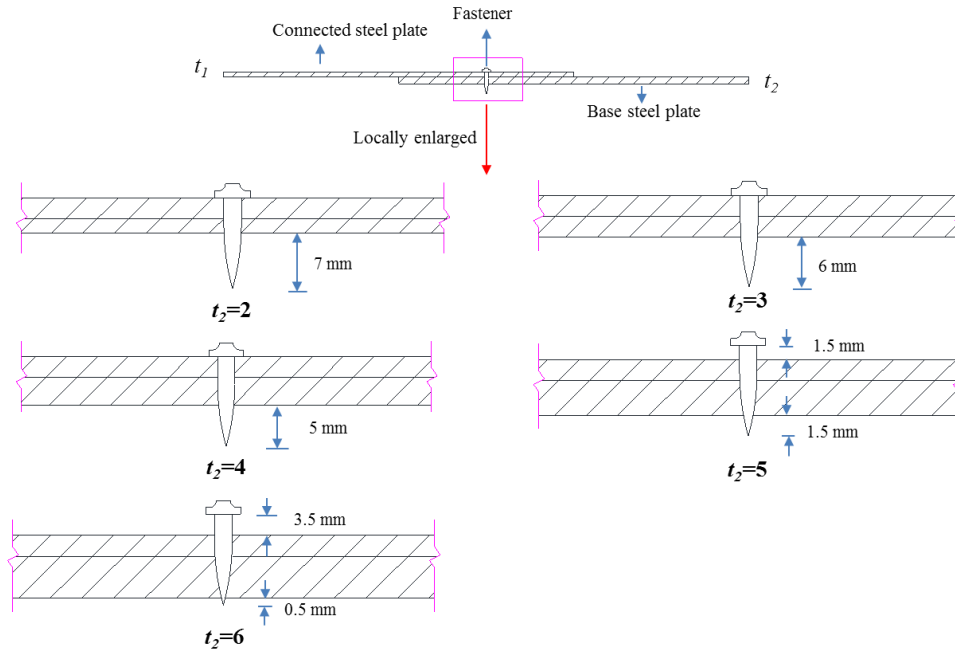
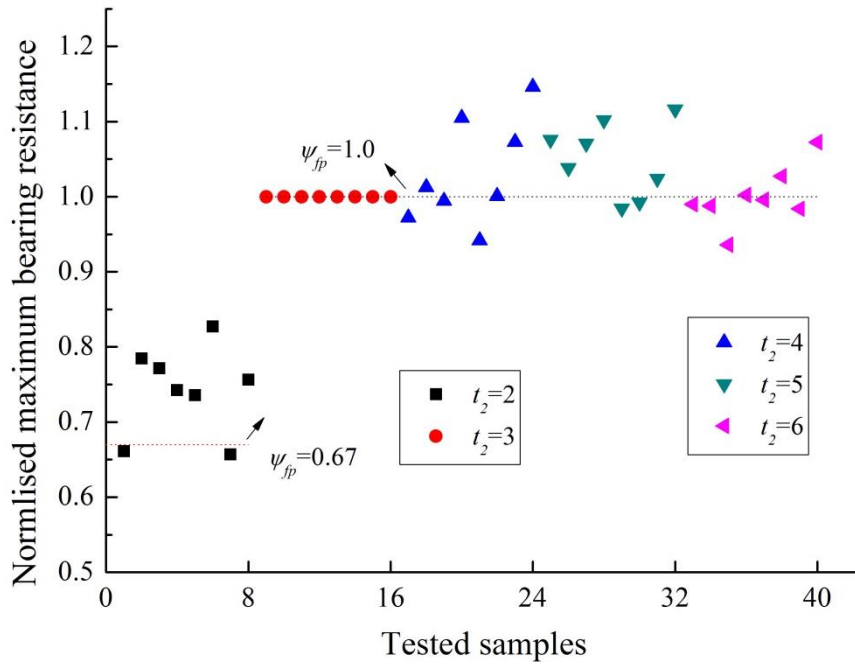
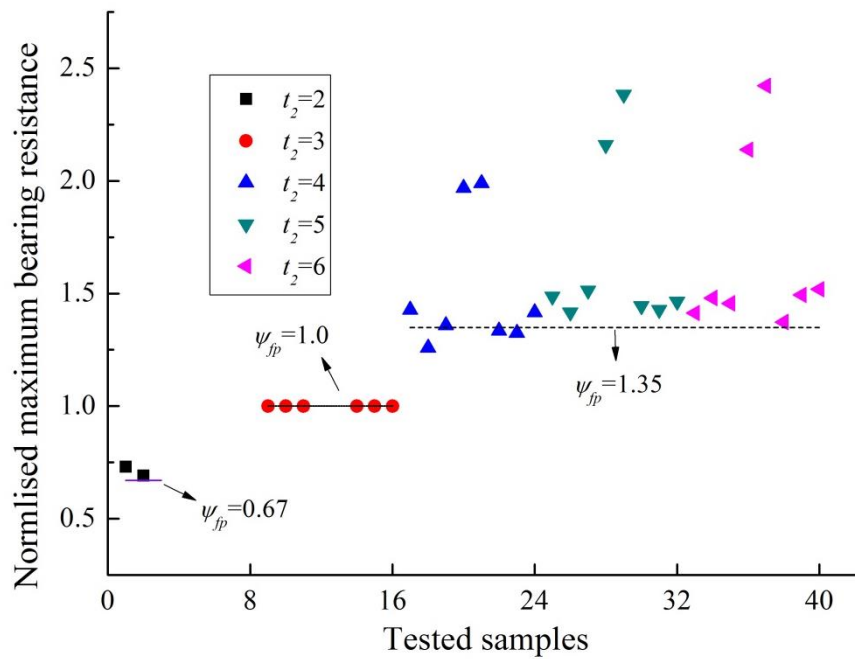


Fig.20. Sample diagrams with different thicknesses of base steel plate



(a)



(b)

Fig.21. Effect of protuberance (a) normalized maximum bearing resistance of samples with pre-drilled holes on connected steel plates and (b) normalized maximum bearing resistance of samples without pre-drilled holes on connected steel plates

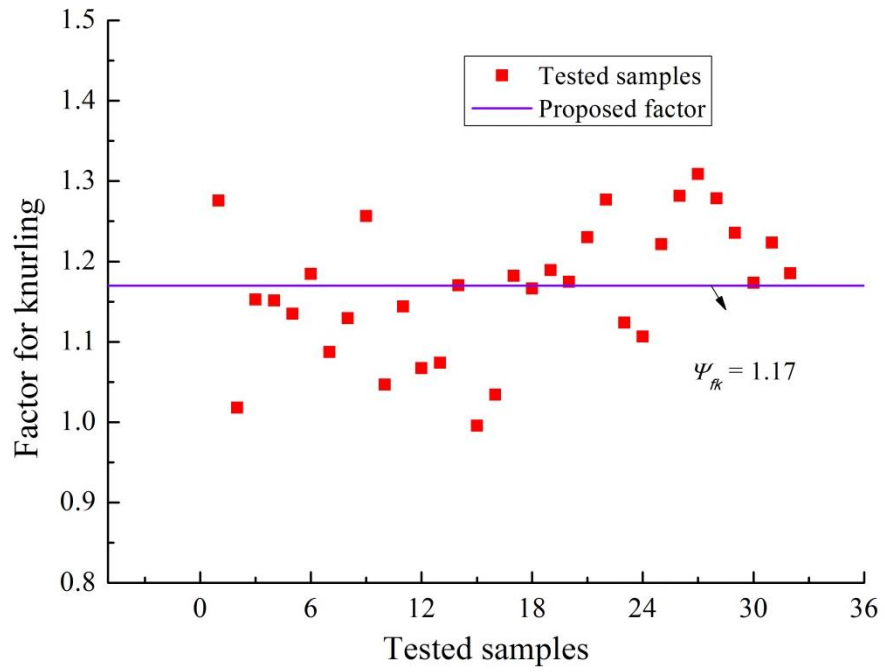
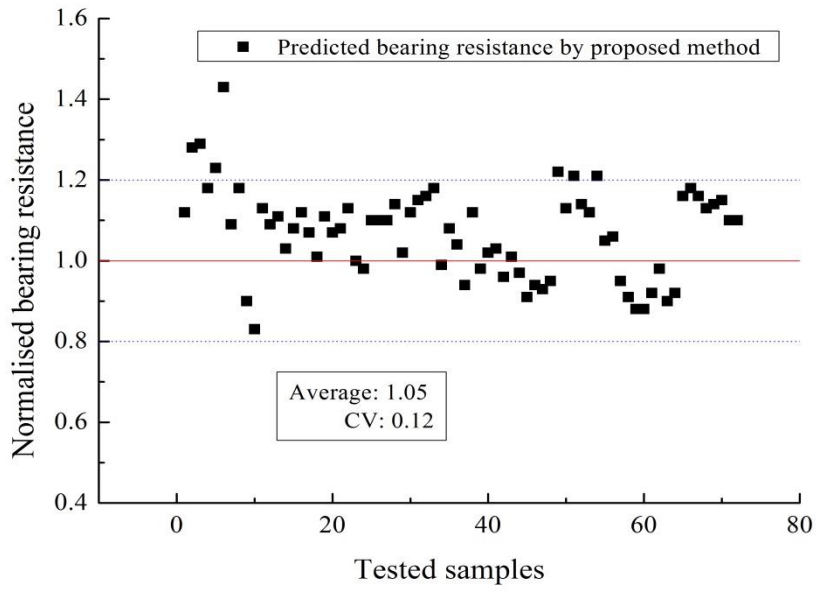
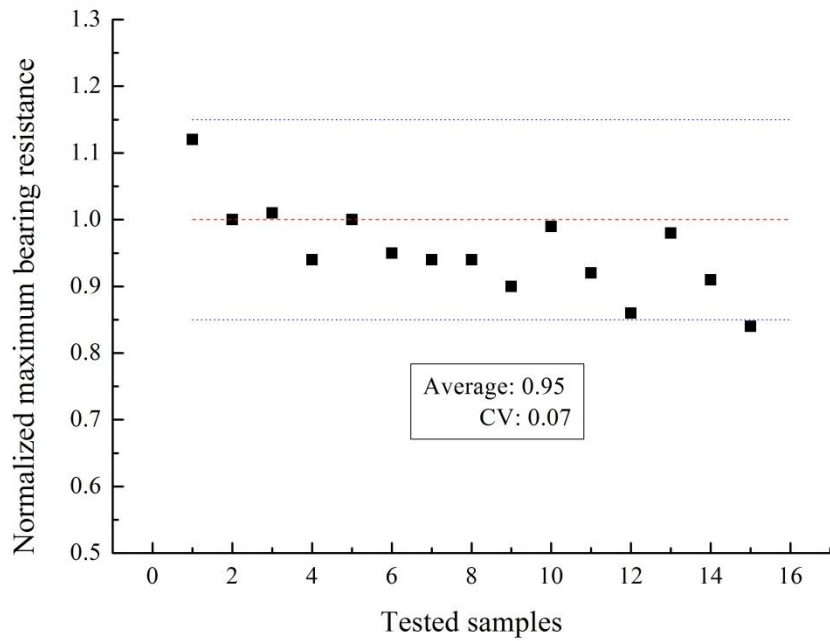


Fig.22. Effect of knurled fastener



(a)



(b)

Fig.23. Verification and validation of the proposed method (a) verification using the data used in factors calibration and (b) validation using the data not appeared in the factors calibration

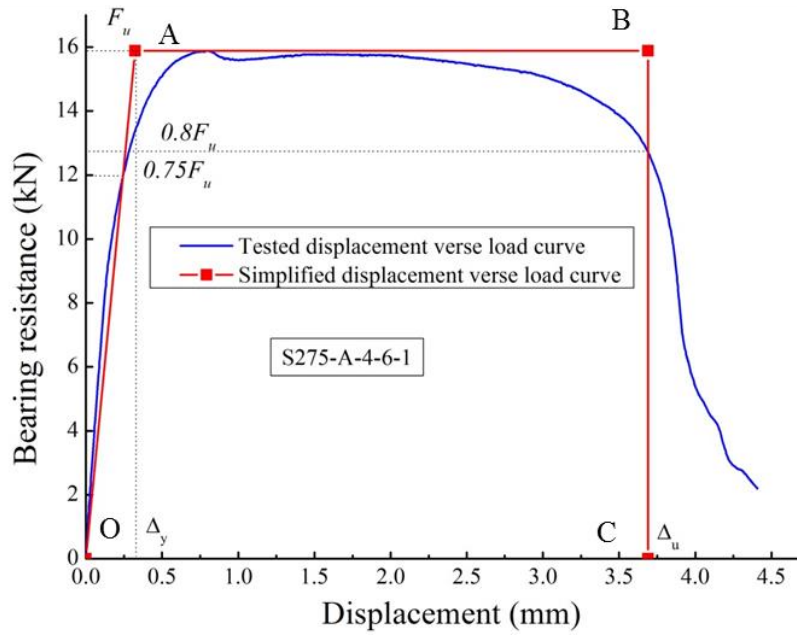


Fig.24. Simple BRVD curve

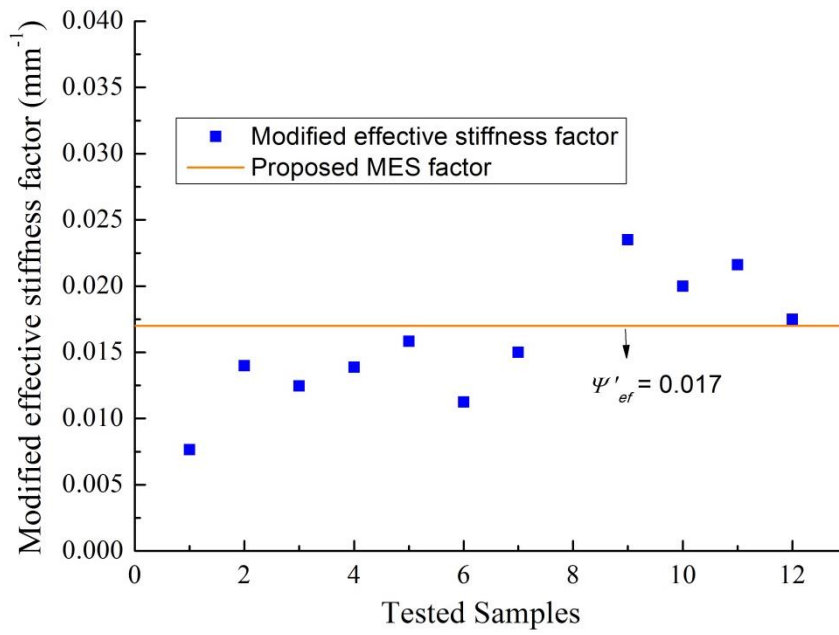


Fig.25. Modified effective stiffness factor

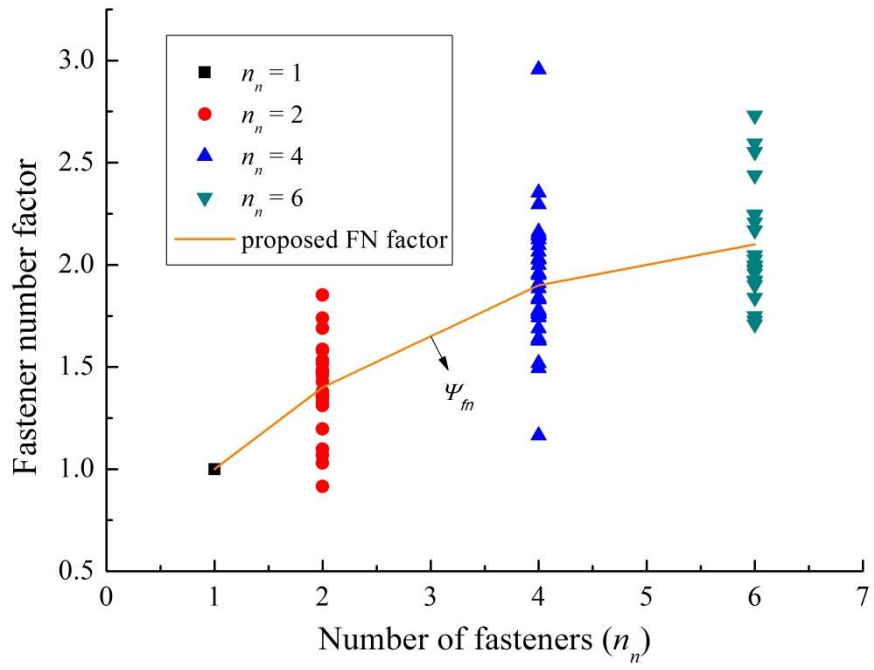
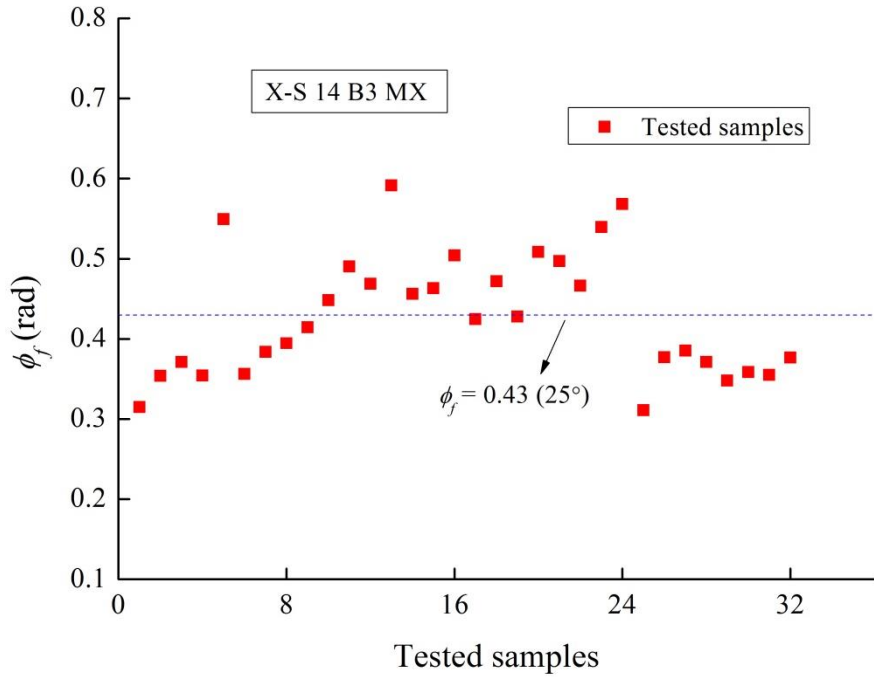
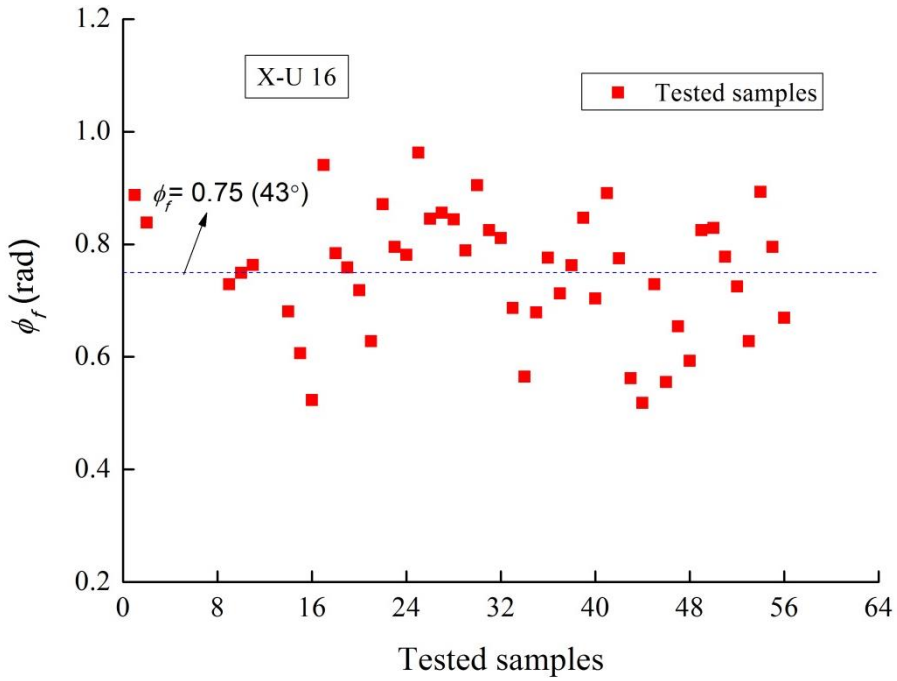


Fig.26. Factor depending on number of fasteners

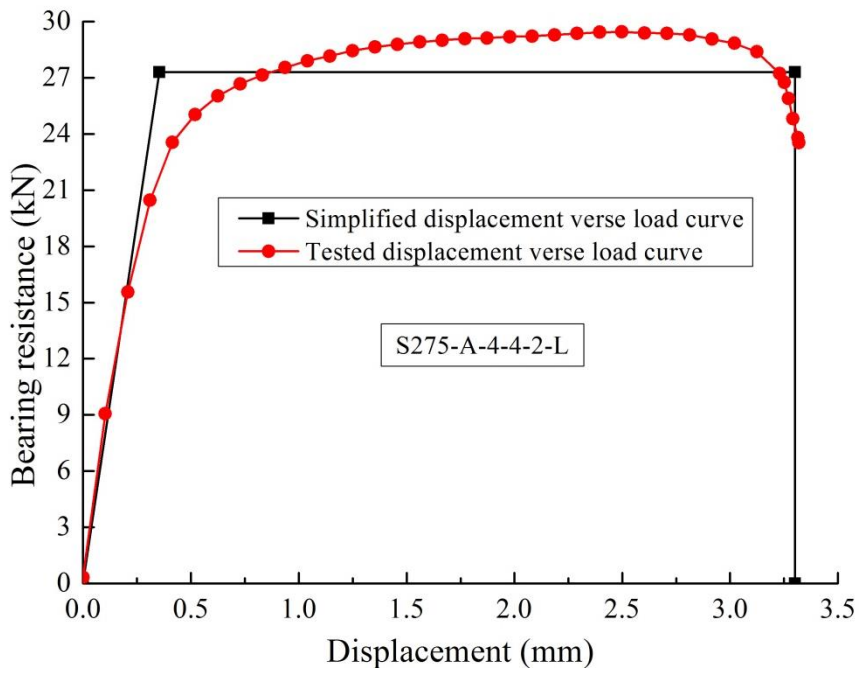


(a)

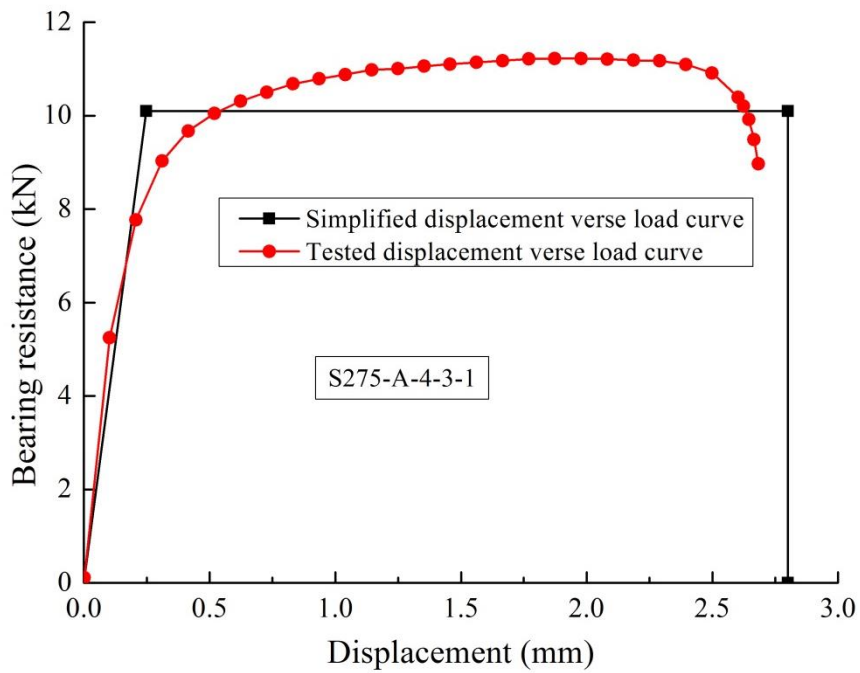


(b)

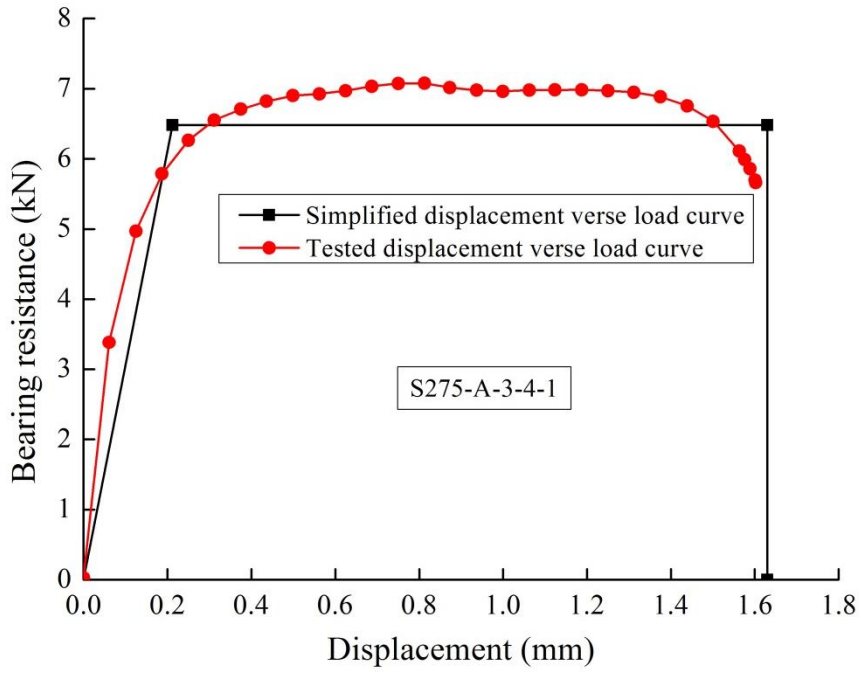
Fig.27. Friction angles (a) fastener without knurling and (b) knurled fastener



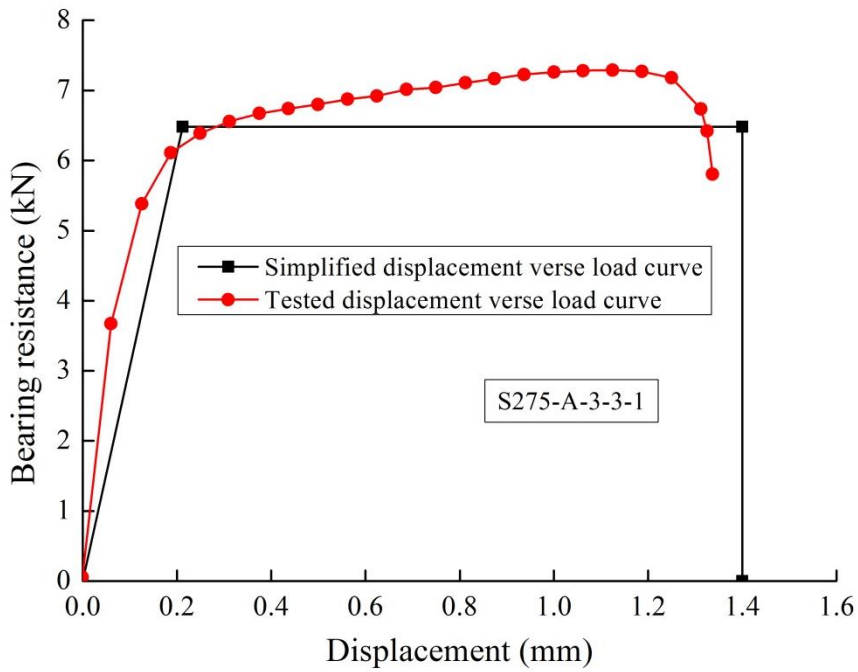
(a)



(b)



(c)



(d)

Fig.28. Comparison between predicted and tested BRVD curve (a) S275-A-4-4-2-L, (b) S275-A-4-3-1, (c) S275-A-3-4-1 and (d) S275-A-3-3-1